

Copyright Warning & Restrictions

The copyright law of the United States (Title 17, United States Code) governs the making of photocopies or other reproductions of copyrighted material.

Under certain conditions specified in the law, libraries and archives are authorized to furnish a photocopy or other reproduction. One of these specified conditions is that the photocopy or reproduction is not to be “used for any purpose other than private study, scholarship, or research.” If a user makes a request for, or later uses, a photocopy or reproduction for purposes in excess of “fair use” that user may be liable for copyright infringement,

This institution reserves the right to refuse to accept a copying order if, in its judgment, fulfillment of the order would involve violation of copyright law.

Please Note: The author retains the copyright while the New Jersey Institute of Technology reserves the right to distribute this thesis or dissertation

Printing note: If you do not wish to print this page, then select “Pages from: first page # to: last page #” on the print dialog screen

The Van Houten library has removed some of the personal information and all signatures from the approval page and biographical sketches of theses and dissertations in order to protect the identity of NJIT graduates and faculty.

ABSTRACT

The depositions of amorphous and cubic-crystal SiC from a new chemical vapor deposition source, diethylsilane(DES), have been studied. Amorphous SiC thin films and crystalline cubic-SiC materials have been deposited on silicon wafers at temperature lower and higher than 850C, respectively. The activation energy and a reaction mechanism involving the production and subsequent desorption of diethylsilene has been suggested, which explains the observed deposition dependency with the temperature and reactor pressure. A model based on the polymerization of DES is offered and the deposition rate is found to be the result of a large number of simultaneously occurring deposition processes for all the polymers involved. The degree of polymerization is thought to determine the uniformity of the deposition rate: if the degree of polymerization is low, homogeneous thin films are deposited; if the degree is high, large thickness variations are observed. Based on the similarity of the pyrolysis of dialkylsilane and silane, DES shows a similar reaction mechanism in the CVD process to silane. A general method of estimation of the kind of reaction mechanism in a CVD process from the kinetics data has been proposed. In an etching study, the Si fraction of the films has been found to be effective on preventing the films from etching. A hypothesis, in which the silicon in amorphous SiC can react with KOH:H₂O etching solution to form a porous film after the etching, has been suggested. In the film evaluation, the films chemical compositions, bonding and crystallinity were determined by RBS, IR and X-ray diffraction, respectively. The IR results show that the hydrogen content in the films can be ignored.

**LOW PRESSURE CHEMICAL VAPOR DEPOSITION(LPCVD) OF
SILICON CARBIDE FROM DIETHYLSILANE**

Master's Thesis

By

Yi-Tong Shi

*Department Of Chemical Engineering, Chemistry And Environmental Science
New Jersey Institute of Technology
Newark, NJ, 07102*

Date: August, 1991

Approval Sheet

**Title: Low Pressure Chemical Vapor Deposition (LPCVD)
of Silicon Carbide From Diethylsilane**

**Name of Candidate: Yitong Shi
Master of Chemistry, 1991**

Thesis & Abstract Approved
by the Examining Committee:

Dr. James M. Grow, Advisor
Associate Professor
Department of Chemistry

Date

Dr. Roland A. Levy, Coadvisor
Professor
Department of Physics

Date

Dr. Reginald. P. T. Tomkins
Professor
Department of Chemistry

Date

New Jersey Institute of Technology, Newark, New Jersey

VITA

Yi-Tong Shi was born in 1960. He earned a B.S. in 1983 from Tianjin University, with a major of Ceramic Science. From 1983 to 1989, he was a researcher in the Research Institute of Chinese National Factory No.798, which is one of the most famous electronic materials companies in China. The accomplished work included uncoated alumina substrates for thin and thick film hybrid circuitries, new ceramic materials as mediums in microwave devices and alumina powder engineering. He attended New Jersey Institute of Technology on September, 1989, receiving a M.S. in Chemistry on October, 1991. The fields of the researches for the M.S. are LPCVD of SiC thin film, wet chemical etching and plasma etching. **Yi-Tong Shi** was awarded Research Assistantship and Teaching Assistantship in NJIT.

CONTENTS

ABSTRACT

LIST OF FIGURESIV

LIST OF TABLESV.

1.INTRODUCTION..... 1

1.1. A Review of Past Work On SiC2

1.1.1.Thermodynamic Equilibrium Considerations in CVD2

1.1.2.Kinetic Studies in CVD6

1.1.3.CVD of SiC Polytypes9

1.1.4.Crack And Other Defects On The Films 11

1.1.5.Wet Chemical Etching14

1.2. Mathematical Model Of LPCVD And Some Important Relations16

1.3. Chemical And Physical Properties Of Organohydrosilanes And An
Expectation Of Their CVD Characteristics18

1.3.1. Similarity of Dialkylsilanes and silane18

1.3.1.1. Pyrolysis of Dialkylsilane and silane18

1.3.1.2. Homogeneous reaction in CVD20

1.3.2. The CVD from Organohydrosilanes21

1.3.3. CVD Source Of SiC and DES23

2. EXPERIMENTAL PROCEDURES

2.1.CVD Apparatus And The Correction Of The Nitrogen Mass Automatic Flow
Controller25

2.2.Procedures For The CVD Study27

3. RESULTS AND DISCUSSION	
3.1. Kinetics And Gas Flow In The CVD	30
3.1.1. Temperature And Activation Energy	30
3.1.2. Gas Flow And Kinetics	30
3.1.2.1.Low Input DES Pressure	38
3.1.2.2.Reaction Mechanism	38
3.2. Polymerization And Its Deposition	44
3.2.1. Homogeneous Gas Phase Polymerization	44
3.2.2. Deposition With The Polymer	45
3.3. Film Evaluation	49
3.3.1. RBS, X-Ray and IR Spectroscopy	49
3.3.2. Optical Microscopic Examination	50
3.4. Etching Study	57
4. CONCLUSIONS	61
5. REFERENCES	62
7. APPENDICES	64

LIST OF FIGURES

Fig.1 The phase diagram for condensed phases in the Si-C-H system	4
Fig.2 Deposition rate versus temperature in the homogeneous reaction model	8
Fig.3 The effect of pressure on the homogeneous reaction	10
Fig.4 Identifying flat on a silicon wafer	29
Fig.5 Temperature dependence of deposition rate	31
Fig.6 Normalized deposition rate versus the position in the reactor at different temperatures	32
Fig.7 Normalized deposition rate versus the position in the reactor at different pressures	33
Fig.8 Normalized deposition rate versus the position in the reactor at different flow rates	35
Fig.9 The relationship between deposition rate and flow rate	36
Fig.10 The relationship between the pressure & deposition rate	37
Fig.11 The relationship between radial thickness variation and pressure	43
Fig.12 The relationship between radial thickness variation and deposition temperature	48
Fig.13 The relationship between chemical composition and deposition temperature	51
Fig.14 The relationship between chemical composition and pressure	52
Fig.15 The relationship between chemical composition and flow rate	53
Fig.16 IR Spectroscopy of the film	54
Fig.17 X-ray diffraction patterns	55
Fig.18 Microstructures of thin film surfaces	56
Fig.19 Microscopic observations after 15-minute KOH:H ₂ O etching	60

LIST OF TABLES

Table 1 The volatility of organohydrosilanes	24
Table 2 Data for the determination of the volume of the CVD chamber	26
Table 3 Factor for DES in N ₂ mass flow controller	27
Table 4 Etching study in "temperature" series wafers	59

LOW PRESSURE CHEMICAL VAPOR DEPOSITION(LPCVD) OF SILICON CARBIDE FROM DIETHYLSILANE

Yi-Tong shi

Department Of Chemical Engineering, Chemistry And Environmental Science

NJIT, Newark, NJ, 07102

1. INTRODUCTION

Silicon carbide(SiC) possesses a unique combination of properties which are not available for other more common semiconductor materials. In addition to its high thermal conductivity and its high melting point, its extreme hardness and its excellent resistance to chemical attack and mechanical damage, SiC is also characterized by a high energy range for its bandgaps (2.2 ~ 3.3ev, depending on the structure type) and a high saturated drift velocity ($2.0 \sim 2.7 * 10^7$ cm/s.). These properties are particularly important for electronic applications.

It is well established that SiC crystallizes into numerous crystallographic structures called polytypes (1,2), which can be described in terms of different stacking orders of Si-C double layers. The only cubic polytype, β -SiC, with the zinc-blende structure, is called 3C in terms of Ramsdell notation. The other polytypes with either hexagonal or rhombohedral symmetries are α - SiC, such as 2H, 4H, 6H, 15R, 21R, etc.

Although early success was achieved in the growth and doping of small SiC single crystal predominantly of the hexagonal 6H polytype via the very high temperature(=2900K) Lely sublimation process (3), the yield of usable crystals was frequently low, their size could not be increased and the energy required to operate the equipment was considerable. Much smaller β - SiC crystals were also produced via reaction of molten Si with the walls of a high purity graphite crucible. However, in this case the product was usually very highly

faulted. Thus, as the technique of chemical vapor deposition(CVD) and the availability of very pure gases improved, investigators increasingly explored and augmented this process to achieve monocrystalline thin film of SiC(4-6).

For about 20 years, silicon carbide produced by CVD has been examined throughout the world as a candidate material for use in specialized applications such as high temperature, high power, or high speed devices. Besides SiC single crystal, CVD provides the possibility that amorphous SiC is formed. In this paper, the author will report a very recent study on SiC thin film deposited by an LPCVD system using a new chemical vapor deposition source, diethylsilane(DES). Before that, a review of the SiC thin film literature and some important relations will be offered. These studies reveal some important methods and an experimental base for the present research. A general discussion about the chemical and physical properties of organohydrosilanes will show why DES was adopted.

1.1. A Review of Past Work On SiC

1.1.1. Thermodynamic Equilibrium Considerations in CVD

The gas composition and possible condensed phase species are functions of temperature, pressure, and source gas composition in a CVD system. The chemical equilibrium calculations involve the computation of the composition of a system, subjected to certain constraints which contains the minimum free energy. The constraints in CVD systems are the preservation of the masses of each element present, constant temperature, and constant total pressure. White et al.(7) initially developed a computational technique which involved the minimization of the summation of the free energies of all the species present in a given system. Erikson(8) extended the method to include systems containing more than one condensed phase, including solid solution, and developed a companion

program(SOLGASMIX-PV) for performing the calculations. This program(or some other similar programs) has been used to calculate the number of moles of the condensed phases which would deposit and to determine the types and amounts of the product gases which would be present under equilibrium conditions. For the system Si-C-H, if the original value of Si/H(or C/H) in the source gas is larger than the thermodynamic equilibrium value , then Si(or C) deposition will occur in going from the initial state to the final one. If the original value is less than the final state, etching of Si(or C) will occur. Single SiC without contamination from the other solid species (C or Si) can only be obtained with the condition that the same deposition rates exists for C and Si.

Harris, Gatos and Witt(9) studied the phase equilibrium by varying silicon and carbon input concentrations at a fixed pressure of 1 atm and constant hydrogen concentration of 0.27 moles in the temperature range from 1300C to 2000C using the above program. The computed compositions of the condensed phases as a function of silicon and carbon input concentrations at 1650C was discussed carefully and is presented in Fig.1. The solid lines delineate three regions as a function of input concentrations(silicon and carbon) in which the vapor phase coexists in equilibrium with one of the following condensed phases: SiC + C, SiC, or SiC + Si. It is of interest to note that single-crystalline deposits of α - SiC were consistently obtained over the whole input concentration range for which SiC is the only thermodynamically stable condensed phase. In the gas phase, there are only five stable silicon vapor species of which four can achieve but negligible concentration; on the other hand, there are more than 20 carbon vapor species of which at least five exhibit significant stability. Thus, significant amounts of carbon can be retained in the vapor phase, whereas very little excess silicon can be accommodated. The presence of many carbon species have essentially a "buffering" effect on the concentration of the carbon constituent. The characteristics are reflected upon the results: (1) The SiC single-phase region only exists in C-rich region. The relative efficiency of silicon carbide, which is defined as Moles SiC/Moles Si in the films, increases with decreasing Si/C ratio. (2) In the phase diagram

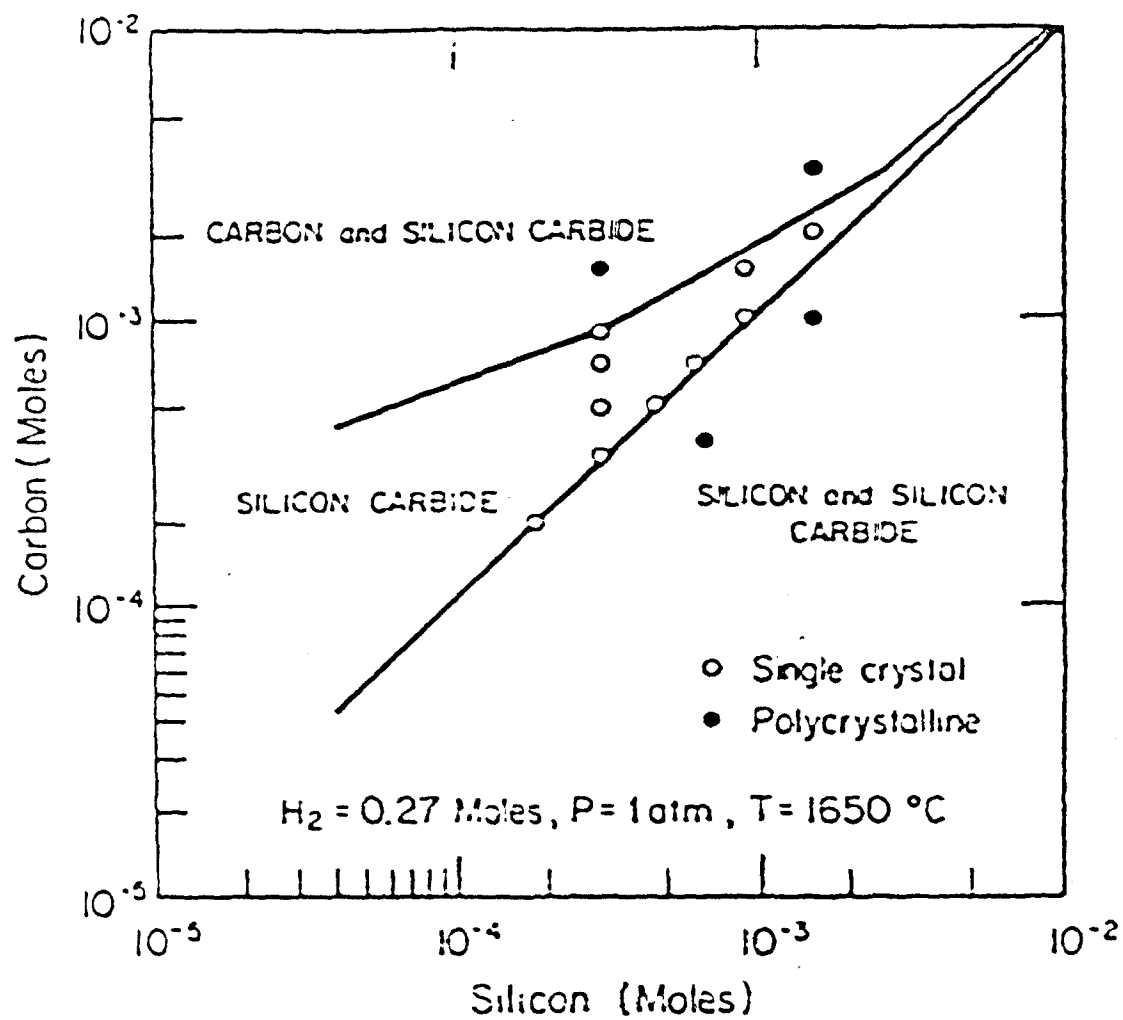


Fig.1. The phase diagram for condensed phases in the Si-C-H system. [9]

for condensed phases given above, the boundary between the SiC single-phase region and the SiC + Si region has a slope of approximately one and an intercept of virtually zero; on the contrary, the boundary between the SiC single-phase region and the SiC + C region has a changing slope (from large to small) with carbon species concentration; that is, silicon vapor-phase species has a constant ability to accommodate the excess of silicon constituent in the whole concentration range. Oppositely, the carbon vapor phase species has a weaker and weaker ability to accommodate the excess of carbon constituent with increasing concentrations of carbon vapor species resulting in the formation of only the SiC single phase. At constant Si/C ratio, higher reactant concentration is suitable for carbon deposition. (3) Consequently, there is a triangle-like narrow region where SiC can be obtained without contamination from other solid species. The lower the input concentration, the wider the region. In other words, single-phase stoichiometric SiC deposition can be achieved at a Si/C input concentration ratio varying from 0.21 to 0.89. At the same time, for lower reactant concentrations with a constant Si/C, the composition of the films is not easily affected by the undulations of the input gas concentrations and only SiC is formed. Finally, temperature dependence of the width of the single-phase silicon carbide region revealed that the relative efficiency of silicon carbide formation decreases with increasing temperature in the range investigated.

Since these results are computed for equilibrium condition they are not expected to apply quantitatively (or in an absolute way) to the open tube growth system. They are generally consistent, however, with the results reported in an earlier paper(10)(in his boundary-layer model of epitaxial growth in an open tube system). The approximation of the results to experimental data obtained under a hot wall CVD (LPCVD) system, as well as for amorphous SiC has not been determined.

1.1.2. Kinetic Studies In CVD

As noted earlier, our principal interest is in an open, flowing CVD system. In order to correctly interpret the phenomena occurring in such a system, one must develop a set of equations that encompasses all phenomena involved to properly describe chemical vapor deposition. This includes a proper representation of reactions in the gas phase, a suitable description of the surface kinetics, and the gas dynamics of the reacting gases. To do this in full generally requires the solution of many coupled, nonlinear, partial differential equations. Such a formulation is clearly beyond the scope of this study and is also not convenient for an applied study.

In fact, CVD processes can be expected to cover a broad range, including completely homogeneous, completely heterogeneous, and intermediate or mixed mechanisms. The author of this paper developed a useful method in which one can estimate what kind of reaction mechanism the CVD process is undergoing, that is, a homogeneous, a heterogeneous, or a mixed mechanism.

In a completely heterogeneous process, a typical mechanism has been given by Claassen, Bloem, Van Den Brekel et al(11,12) for the deposition of Si from SiH₄. The kinetics equation possesses the form

$$\text{Deposition Rate D.R.} = \frac{a P}{1 + bP} \quad (1)$$

the temperature dependence of deposition rate follows an exponential law:

D.R. $\sim \exp(-E_a/kT)$ at low temperature and the deposition rate is essentially independent of temperature at high temperature.

In a homogeneous reaction model, the substrate serves only as a site for condensation of the solid product. For this case, single molecules of the solid product will form in the gas

phase reaction, diffuse to the substrate and undergo condensation to form a film. There is, however, a competing process which can cause powder formation in the gas phase. If the gas phase concentration is too large, the rate of collision of molecules will be appreciable. This will lead to the formation of polymers in the gas phase, or, in other words, to powder formation. Sladek (13) considered the effect of temperature on homogeneous reactions theoretically. At low temperature, the powder formation is negligible. For this condition, the deposition rate also follows an exponential law: $D.R. \sim \exp(-E_a/kT)$. As temperature increases, the rate of dimerization of the reactant becomes comparable with the rate of film formation. Dimers are followed by larger clusters, and at higher temperatures most of the reaction product is in the form of particles rather than film. The transition from film to particles formation occurs rather suddenly at a critical value, T^* . When the temperature is beyond the critical value, the deposition rate decreases rapidly, which is different from that in the heterogeneous process. A typical deposition rate-temperature curve is sketched in Fig.2. Homogeneous reactions are favored at higher temperature than heterogeneous reaction.

Furthermore, the following example reveals the effect of pressure on a homogeneous reaction, which is different from that on heterogeneous process. Kim, Edmond, Ryu, Kong, et al.(14) deposited β -SiC epitaxial thin films on Si (100) substrates in a cold wall, barrel-type reaction chamber by using the high-purity gases, silane (SiH_4) and ethylene(C_2H_4) at temperature of 1387C and found the growth rate increases with the increase in the Si/Si+C ratio up to Si/Si+C =0.496, then the growth rate is rapidly reduced beyond Si/Si+C=0.5. At the same time, as the Si/Si+C ratio was decreased below 0.5, black inclusions, which are SiC particles, appeared in the β -SiC films and increased in size and density as the amount of C in the gas phase increased; however, numerous spherical particles occurred in the β -SiC film growth at Si/Si+C =0.535 which were not observed at lower values of this ratio. Unfortunately, these investigators did not give an exact reason for this phenomenon. However, a possible explanation for these experimental results can

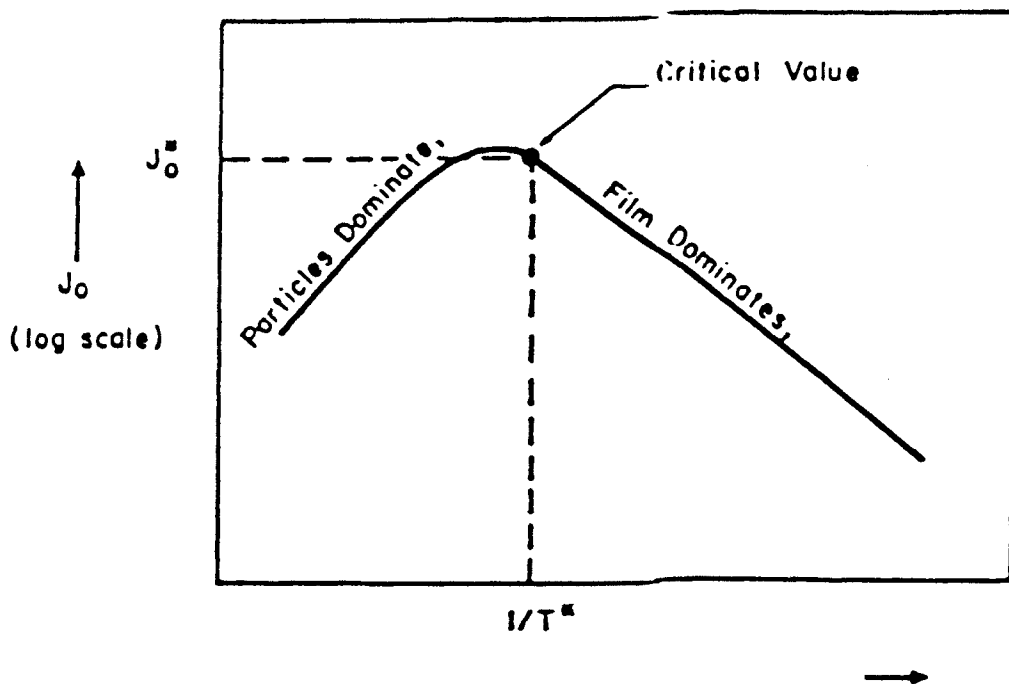


Fig.2. The curve of deposition rate versus temperature in a homogeneous reaction model. [13]

be obtained by applying the theory of homogeneous reaction. It can be believed that the particles produced at $\text{Si}/\text{Si} + \text{C} = 0.535$ are Si which the thermodynamic calculations predict should be produced in this range and was formed by polymerization in the gas phase. Furthermore, their residence time in the gas phase may allow them to serve as sites for the additional heterogeneous nucleation and growth of Si which would normally be used in the reaction with C_2H_4 to form SiC. At the constant total pressure, the polymerization of SiH_4 can be ignored when the ratio of $\text{Si}/\text{Si} + \text{C}$ is much less than 0.5; but the effect is important when the ratio is high. At the $\text{Si}/\text{Si} + \text{C}$ ratio range of 0.496 - 0.500, the thermodynamic calculations reveal that the condensed phase is SiC only and the partial pressure is higher than the critical value, that is, the polymerization of silane occurred(12). As a result, black inclusion, or SiC particles, appeared in the SiC films. At the same time, the growth rate is rapidly reduced beyond $\text{Si}/\text{Si} + \text{C} = 0.5$ because the silicon powder formed by the homogeneous reaction results in the depletion of the reactant gas. Fig.(3) shows the effect of pressure on the homogeneous reaction from experimental results.

Thus, we can estimate the reaction mechanism in CVD according to the experimental kinetic data and the comparison with the typical kinetics formula described above. The present study will demonstrate the application of the method.

1.1.3. CVD of SiC Polytypes

Obviously, the computation described in section 1.1.1. gives no information as to how the condensed phases physically coexist, which polytypes are formed, and whether or not β -SiC appears in single-crystal or polycrystalline form.

The controlled growth of SiC single crystals giving a preselected polytype has been studied. Yoshida (15) reported that monocrystalline β -SiC and 6H-SiC were grown on 6H-SiC at low (1330- 1500C) and high temperatures(1700-1800C) respectively; on the other hand, on 3C-SiC, β -SiC was grown up to 1800C, at which temperature 6H-SiC was grown.

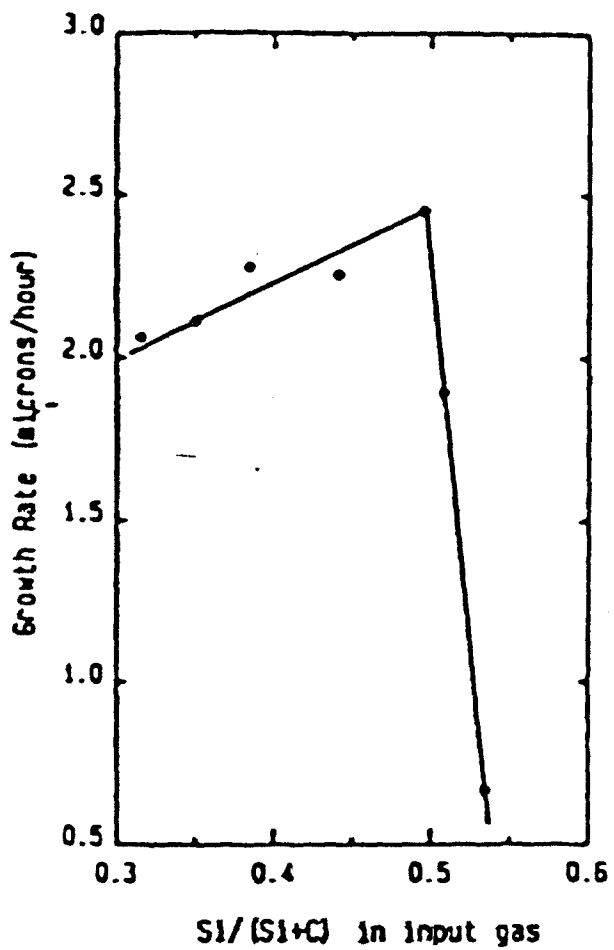


Fig.3. The effect of pressure on a homogeneous reaction from experimental results. The total pressure is constant. [14]

The films were deposited in a horizontal, water-cooled, quartz reaction tube using a silane-propane mixture and hydrogen as the carrier gas. In the same reactant gas system, Powell(16) deposited β -SiC on (100)Si substrates at 1360C which was higher than the CVD reactor temperatures on SiC substrates. Liaw et al(17) used an RF heated cold-wall barrel-type CVD reactor with SiH₄-C₂H₄-H₂ to deposit β -SiC on (100) and (111) Si substrates at temperatures of 1310C and 1327C, respectively. However, Furumura et al(18) obtained their β -SiC films on a Si off-axial (111)substrate from another reactant gas system SiHCl₃-C₃H₈-H₂ at temperature as low as 1000C. Obviously, the controlled growth of SiC single crystals having a preselected polytype has a strong dependence on substrates, the orientations, reactant gas system used, and CVD reactor temperatures. From Raman Scattering studies in CVD, β -SiC on (100)Si(19), CVD grown β -SiC films on Si possess the same crystalline orientation as the Si substrates.

The attainment of single crystallinity in the films is controlled by chemical composition of the films(20), reactor temperature(17) and the surface characteristics of the substrates(21). Monocrystalline SiC can grow only stoichiometrically [with a maximum deviation of 10^{-5} atomic per cent (a/o) from stoichiometry] and enough reactor temperatures (17); otherwise, polycrystalline forms.

Although the term "amorphous" has negative connotations, it should be noted that many electronic products incorporate amorphous semiconductors. Some technologies are not possible with crystalline materials(22). Amorphous SiC has been produced by plasma CVD, but not by APCVD or LPCVD(23).

1.1.4. Crack and other defects on the films

Crack-free monocrystalline SiC films having a very smooth final surface have been one of the major objectives in many CVD laboratories all over the world. Si has been the substrate commonly chosen because it is readily available and also because it is one of the components of the final product. However, the 8% and 20% mismatch in the

coefficients of thermal expansion and lattice parameters, respectively, of these materials did not previously allow the thickness of the films to exceed 2 μ m without considerable microcracking on cooling. An extensive study of defects in SiC on Si substrates and the amelioration of the mismatches have been reported mainly by Fatemi, Nordquist, Liaw, Davis, Nishino et al. (17,24). According to their work, the formation of crack-free monocrystalline SiC films having very smooth final surface requires:

(1) No possibility of defect formation, due to stress propagation and the tendency of polycrystalline on the films, that is, deposition of No-defects and uniformity, less off-axis orientation on the surface of the substrates, proper Si/C input concentration ratio and high enough temperature must be met;

(2) A uniform buffer layer, which reduces the stress between the films and substrates;

(3) Optimal thickness of the "buffer" layer, in which the crystal field(24) of the substrate can be through the buffer layer. For example, if the buffer layer is polycrystalline, the buffer layer should be especially thin so that the growth of single crystalline SiC can be controlled by the crystal field of Si substrates and the reactor temperature should be increased.

The amelioration of the mismatches in expansion coefficients and lattice parameters is based on a two step CVD process whereby a "buffer" or "converted" layer is initially formed on a Si substrate surface via different methods before the growth of thin films of β -SiC. By introducing an intermediate layer as a buffer layer, stresses caused by the mismatches can be released.

For example, Liaw and Davis obtained crack-free monocrystalline β -SiC film having a very smooth final surface at 1327C and 760torr on (100)Si substrates using SiH₄ and C₂H₄ on an RF heated cold-wall barrel-type CVD reactor, when the Si wafer is initially reacted with the C₂H₄ alone. Scanning electron microscopy was used to characterize both the chemical conversion process and the growth of the β -SiC thin film: if the chemical conversion proceeded under isothermal conditions, that is, 1327C, the conversion produced

relatively large localized deposits of carbon, being rectangular on the (100)Si substrates. It is believed that these areas acted as nucleation sites for the subsequent CVD, as the β -SiC films tended to be polycrystalline with very rough surfaces. By contrast, heating the Si substrates from room temperature to 1327C in flowing C_2H_4 in H_2 at 760 torr produced thin but much more uniform deposits. The study also revealed that defects on the Si substrates can extend to the surfaces of the converted layer as well as the final films. The third result is that the final surface of the films on (100)Si having 1 off-axis orientations, was very smooth; however, films grown on a wafer with 6 off-axis orientations had a moderate and very rough appearance. The work concluded that with the non-defect substrate, less off-axis orientation and uniform chemical conversion by initially flowing a carbon-containing gas and a carrier-gas alone are the key steps in the formation of crack-free monocrystalline SiC films having a very smooth final surface.

Liawand, Davis, Nishino et al used a sputtering method in which an intermediate layer of β -SiC was prepared. The key step is that the thickness of the sputtered layer must be less than 100um. It is speculated that the growth of the single crystalline β -SiC was controlled by the crystal orientation of the Si substrate through a polycrystalline intermediate layer formed by sputtering. The advantages of a sputtered SiC intermediate layer arises from the comparison with the one obtained by CVD. In the CVD system, the ideal grown layer is formed under a condition of thermodynamic equilibrium, so that nucleation and growth are strongly dependent on the surface treatment of the substrates. The initial stage of growth is influenced by parameters difficult to control, such as surface roughness and dislocations. An adatom moves toward favorable sites of the substrates, so the density of nucleation on the surface might be nonuniform atomically. As a result, single crystal growth of β -SiC on a Si substrate by the CVD process needed careful preparation including SiC coating of the susceptor and etching of the substrate before the crystal growth. Furthermore, reproducibility of single crystal growth was not good. In the sputtering method, deposition is carried out under a nonequilibrium condition. Sputtered

atoms uniformly hit the whole area of the substrate and nucleation may occur more uniformly over the surface. The intermediate layer of β -SiC prepared by sputtering can be more uniform than that by CVD. Consequently, the initial stage of growth in the subsequent CVD process is not strongly dependent on the surface and single crystals of β -SiC are reproducibly obtained.

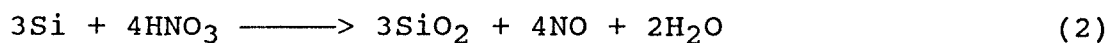
The crystalline quality may depend on variations in the impurity or doping concentrations as a stress-relief mechanism. These possibilities also are presently under investigation.

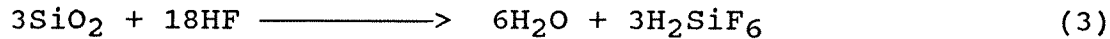
1.1.5. Wet Chemical Etching

Monocrystalline SiC has proved to be strongly resistant to chemical attack. With the exception of slow decomposition in hot H_3PO_4 , no acids and bases are known to chemically attack crystalline SiC(25). The application of the etching systems based on acids (for example, $\text{HNO}_3 : \text{HF} : \text{H}_2\text{O}$) or bases (for example, $\text{KOH} : \text{H}_2\text{O}$) upon the monocrystalline SiC film deposited on Si wafers has shown promise in two general areas: the evaluation of the SiC films and the use of SiC films as etching masks.

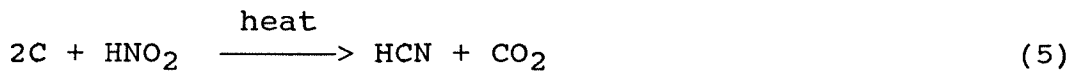
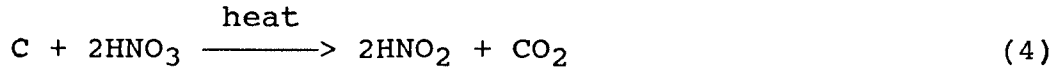
In amorphous SiC, however, the Si and C are more weakly bound to each other than in crystalline SiC. Furthermore, the material possesses a much more open structure and contains a high concentration of dangling bonds. As such, the kinetics of the etching process are enhanced.

For example, Edmond, Palmour, and Davis(26) studied the chemical etching of ion implanted amorphous SiC in the (1:1)HF:HNO₃ system and concluded that crystalline SiC does not react with (1:1)HF:HNO₃. However, amorphous SiC reacts completely and readily in this acid solution at temperature more than 45C. All of the Si in the amorphous SiC dissolved according to the reaction





and all of the C in the amorphous SiC dissolves most probably by the following set of reactions:



Amorphous thin SiC films produced by implantation of P or Al etched at a rate equal to 100nm/min, whereas those produced with a combination of Si and C implants etched at a rate equal to 250nm/min. It should be noticed that pure Si can react with the etching solution at room temperature by the same reaction equation and pure C can react with the etching solution by the same reaction equation only when the temperature is higher than 45C. Furthermore, a layer of pure carbon can be observed after the amorphous SiC is immersed into the etching solution at room temperature and the layer stops the etching. If the temperature is increased to 45C or the C-layer is wiped away, the etching goes on.

The work strongly suggested that the open structure and high concentration of dangling bonds have made the Si or C in amorphous SiC behave like in pure Si or C to some degree.

Unfortunately, the wet chemical etching of amorphous SiC in the KOH:H₂O system has not been studied. The present work will report some interesting results on this topic.

1.2. Mathematical Model of The LPCVD System And Some Important Relations

For the convenience of the following discussion, a review of the mathematical model of the LPCVD system is necessary. In this section, the discussion about the model is based on the work of Middleman and Yeckel(27) in which the following assumptions are made:

- (1) The wafers are stacked axially within a tubular reactor,
- (2) Symmetry is assumed about the axis of the reactor. Asymmetry can arise from the geometry of the wafer boat, and the effect is believed to be minor in comparison to the major issues of the model,
- (3) Only a single chemical species need be considered,
- (4) The gas contains that species with low pressure or highly diluted in an inert carrier gas ,
- (5) Only heterogeneous reactions need be considered and the reaction rate is first order in reactant,
- (6) There is no flow in the interwafer region.

With the pure diffusion analysis, the mathematical model and the solution (that is, the concentration distribution) have been obtained. However, the useful features for this work are some other results from the solution of the model. Those results will be discussed as follows.

1.2.1. Uniformity of Deposition

Various measures of uniformity can be defined. One could, for example, take the difference between the minimum and maximum deposition rates and normalize that difference to the mean deposition rate which is approximately equal to the average value of the minimum and maximum deposition rate. Mathematically, the uniformity can also be expressed by the radial thickness variation:

$$\text{Variation}[\pm] = 100 * (d_{\max} - d_{\min}) / (d_{\max} + d_{\min}) \quad (6)$$

If the dimension of the wafer and the interwafer spacing are fixed, the uniformity reveals a strong dependence on the Sherwood number, Sh , which is defined as:

$$Sh = k_D d / D \quad (7)$$

where k_D is the mass transfer coefficient of the process, d is a relevant length dimension and D is the diffusion coefficient of the reactive compound. When Sh is less than unity, the deposition process is surface controlled; when Sh is greater than unity, the deposition process is diffusion controlled. Specifically, if Sherwood numbers are below 10^{-3} , which can be achieved with ease, the uniformity of the deposition rate is obtained and the radial thickness variation can be ignored.

1.2.2. Mass transfer coefficient and some relations

In an LPCVD system, the reactive species can adsorb and then decompose upon impacting the surface. This is a heterogeneous surface reaction which can be described in terms of the mass transfer coefficient, k_D . The mass flux can be expressed as follows:

$$J = \frac{k_D}{RT} (p - p_{eq}) \quad (8)$$

where p_{eq} is the partial pressure of species i that would exist under equilibrium at the surface temperature, k_D is the mass transfer coefficient and p is the pressure in the LPCVD system.

If the deposited layer mass in unit time is defined as the deposition rate, D.R.,(or growth rate, G), the formula (8) can be changed to:

$$D.R. = \frac{S k_D}{RT} (p - p_{eq}) \quad (9)$$

where S is the surface area of one wafer. We differentiate D.R. with respect to pressure p and obtain:

$$\frac{d(D.R.)}{dp} = \frac{S}{RT} k_D \quad (10)$$

which means the value dG/dp is proportional to the mass transfer coefficient, k_D . This relation will be applied to this study.

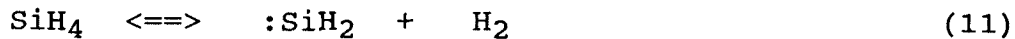
1.3. Chemical and Physical Properties Of Organohydrosilanes And An Expectation Of Their CVD Characteristics

1.3.1. Similarity of Dialkylsilanes and silane

Dialkylsilanes are derivatives of silane with alkyl substituents. A comparative study between dialkylsilanes and silane is necessary for better understanding the characteristics of these kinds of materials in CVD.

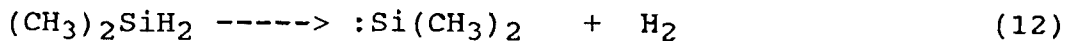
1.3.1.1. Pyrolysis of Dialkylsilane and silane

Various researchers have reported on the homogeneous decomposition of silane(SiH_4) and the occurrence of $:\text{SiH}_2$ radicals. Newman et al(28) concluded that the initiation reaction of the homogeneous decomposition is

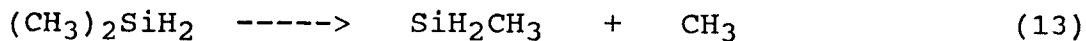


The silylene is considered to be adsorbed over the surface to a kink position in a CVD process and a model, in which the adsorption mechanism is determined to limit the deposition rates, has been obtained. The model is quantitatively in agreement with the experimental data(11,12).

Similarly, it has been determined that the primary decomposition pathway for dialkylsilanes involves silylene formation by extrusion of H₂. The pyrolysis of dimethylsilane (DMS) provides an example(29):



Primary decomposition pathways involving homolytic cleavage of silicon-carbon bonds are negligible at temperature below about 725C, but can be important at higher temperature(29).



and the temperature of homolytic cleavage of silicon-carbon bonds will decrease with the increase of the length of the alkyl.

Thus, we can propose for the surface process in CVD that the silylene (R₁R₂Si:) will be adsorbed on the substrate surface at low temperature, an adsorption mechanism is expected to be a limitation for the deposition rate and the kinetic equation should be similar to that of silane(11,12). However, the details of reaction mechanism will change at

high temperature, that is, Si-C bond homolysis becomes important. The temperature depends on the length of the alkyl substituents. The longer the substituents, the lower the temperature.(29)

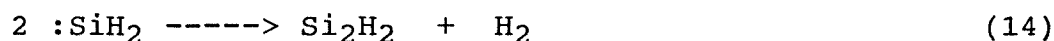
1.3.1.2. Homogeneous reaction in CVD

The homogeneous reaction for polymerization of silane has been studied carefully by some investigators.

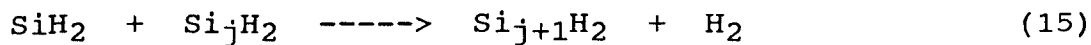
Van den brekel and Bollen(12) detected the formation of silicon polymers by means of mass spectrometry and by laser light scattering in the temperature range of 625-725C in the LPCVD system. Large clusters with monocrystalline character have been observed in the gas system. Electron microscopic investigations of the clusters revealed the presence of a size distribution of monocrystalline silicon particles having a diameter between 50 and 100 A. Such large particles contain 10^4 and 10^5 silicon atoms.

Furthermore, Murthy et al(30) investigated the polymerization of silane in a conventional horizontal epitaxial reactor consisting of a resistance heated quartz tube. They have ascertained that fine crystallines of silicon can be obtained when the input silane concentration exceeds a critical value dependent on temperature. By electronmicroscopy, the size, shape and structure of the particles have been determined: the particles were found to be single crystalline and mostly defect free with three kinds of crystal habits(Octahedral, Tetrahedral, and Truncated triangular bipyramidal), the most common being octahedral. The size distribution of monocrystalline silicon particles has a diameter between 300 and 800A. The polymerization must be considered as the growth of silicon atoms on a nucleus.

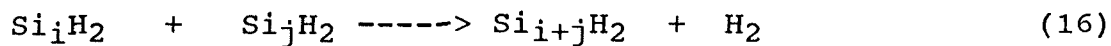
Newman et al.(28), who studied the initial reaction of the decomposition of silane, proposed a mechanism for the dimerization process:



Based on the same principle, Van den brekel and Bollen(12) suggested further polymerization reactions in which silylene reacts with a j-mer, Si_jH_2 , under elimination of molecular hydrogen:



as well as the combination of two polymers:



The polymerization mechanism satisfactorily explained that radial growth rate variations of polycrystalline Si deposited by using a SiH_4 source(12).

Based on the similar principle, the author of the present work expects diethylsilanes to polymerize at some conditions and proposes a mechanism for the polymerization process or homogeneous reaction. As a result, obvious radial thickness variation and some homogeneous reaction effect on the kinetic equations are expected to occur for polymerization. The detailed discussion will be offered in section 3.2.

1.3.2. The CVD from Organohydrosilanes

Dialkylsilane and silane have been determined to decompose through homolytic cleavage of the two Si-H bonds and subsequent radical formation(29,31). As a result, the

silylenes have been suggested to be adsorbed on the substrate surface and an adsorption mechanism, or a heterogeneous process, has been proposed. In addition, the polymerization processes based on the combination of the silylenes are suggested in order to explain the radial thickness variation and homogeneous reaction effect.

The following data and experimental results support these models described above and help give a general picture of the CVD of organohydrosilanes.

(1) The bond of Si-H is the weakest of the bonds of Si-H, Si-C, Si-Cl and C-H(31). The percent decomposition (that is, the homolytic cleavage of the two Si-H bonds) versus temperature profiles for members of the dialkylsilanes and silane are similar, with decomposition beginning at 460-480C and ends at 625-725C. It is interesting that the polycrystalline Si film from SiH₄ or SiH₂Cl₂ is deposited at 625C and 690C, respectively ; and the amorphous SiC from DES is produced at 600-800C. However, the depositions of polycrystalline Si from SiHCl₃ and SiCl₄, which can not result in the silylene radical, occurs over 750C - 850C temperature range.

(2) In the depositions from silane and DES, the radial thickness variation occurs; however, the deposition from SiCl₄ results in the uniformity of the films, that is, no polymerization has been found. These experimental results on the radial thickness variation strongly support the model of polymerization as will be expressed in section 3.2.

As a hypothesis, a general picture of the CVD of organohydrosilanes can be expected:

(1) In organohydrosilanes, dialkylsilanes (R₁R₂SiH₂) can form silylenes (R₁R₂Si:) at a low temperature range(30,32). The decomposition begins at 460-480C and ends at 625-725C. Over the range of temperature, the homolytic cleavage of silicon-carbon bonds can not be negligible. The other kinds of organohydrosilanes do not possess the decomposition pathway.

(2) The formed silylenes(R₁R₂Si:) is adsorbed in the substrate surface and a heterogeneous process occurs. The mechanism expressed in section 3.1.2.2. can be

considered to be typical. As a result, the process possesses a lower activation energy than in the other kinds of organohydrosilanes.

(3) All of dialkylsilanes are expected to polymerize with a similar pathway, however, the effect of polymerization will decrease with the increase of the length of substituent alkyl because of the volume effect described below.

(4) In dialkylsilanes, the longer alkyl substituent is expected to result in lower activation energy than shorter alkyl substituent because the formula (24) is rate-limiting in the reaction mechanism (This will be discussed later). However, volume effect in collisions of molecules (or radicals) or adsorption on a substrate surface resulted from the length of the alkyl will become important when the alkyl is long. In kinetics, the effect will result in a lower effective probability factor in a longer alkyl substituent than in a shorter alkyl substituent.

(5) Because the temperature of the homolytic cleavage of a silicon-carbon bond will decrease with the increase of the length of the alkyl substituent in dialkylsilane, the kinetic characteristics are expected to become complex when the substituent alkyl increases in length.

1.3.3. CVD Source Of SiC and DES

As was described above, some requirements must be met for the CVD source of SiC. In the past work, SiH₄ has been used for the synthesis of SiC. However, SiH₄ is a toxic, pyrophoric, potentially explosive gas which requires expensive installations to meet the safety standards. In addition, high temperature is required, the carbon-containing gas must be used and no amorphous SiC can be formed, which are limited in many applications. However, DES shows attractive advantages in the synthesis of SiC by CVD according to the following discussions.

In organohydrosilanes, methyl ligands required a higher pyrolysis temperature than higher normal alkyl homologues. That means that the organohydrosilane with a large alkyl ligand has lower deposition temperature. However, the volatility will decrease with the increase of the length of the alkyl so that the delivery system for CVD becomes complex. The reduction in the number of alkyl, i.e. the substitution of an organic moiety by hydrogen, also leads to lower deposition temperature sources. This is accompanied by a higher volatility and higher Si/C. Table 1 shows the boiling points of different organohydrosilanes. DES has the suitable ratio Si/C = 0.25 (in the carbon excess region) and vapor pressure (200 torr at 21°C), which make it possible that the use of delivery by commercially available gas mass flow controllers without the need for heated lines. Furthermore, purified DES is non-pyrophoric and non-toxic and doesn't require expensive installations to meet the safety standards.

Compounds	Name	Boiling point (°C)
H_3SiCH_3	Methylsilane	-57
$\text{H}_3\text{SiC}_2\text{H}_5$	Ethylsilane	-14
$\text{H}_3\text{SiC}_4\text{H}_9$	Butylsilane	56
$\text{H}_3\text{SiC}_6\text{H}_{13}$	Hexylsilane	114-115
$\text{H}_2\text{Si}(\text{CH}_3)_2$	Dimethylsilane	-20
$\text{H}_2\text{Si}(\text{C}_2\text{H}_5)_2$	Diethylsilane	56

Table 1. The volatility of organohydrosilane

In this study, the suitability for the LPCVD system has been determined. The kinetic study yielded many interesting results.

2. EXPERIMENTAL PROCEDURES

2.1 CVD apparatus and the correction of the N₂ mass automatic flow controller

The CVD experiments were carried out in a LPCVD reactor, consisting of a fused quartz reactor tube, having an inner diameter of 12.5 cm and a length of 120cm, mounted within a three-zone Lindberg furnace. The apparatus was equipped with a WS 250 roots blower backed by a D30AC vacuum pump from Leybold-Heraeus. The reactor pressure is controlled with a manually controlled valve. The reactor temperature was measured by an Omega type K thermocouple. Gas flows were regulated by an automatic N₂ mass flow controller which was corrected for DES and will be described in detail below. The pressure in the reactor was measured with a 10 torr maximum baratron gauge from MKS.

Six boron-doped monocrystalline silicon wafers from SEH Corporation, oriented on (100) and 10 cm in diameter, were placed in an upright position about 110° with respect to gas flow direction, on a fused quartz boat, in such a way that the axis of the row of slices coincided with the tube axis. The wafer spacing used was normally 3cm. The polished side was directed to the upstream end on the reactor tube.

In this study, an automatic N₂ mass flow controller was used to determine the flow rate of DES vapor because there is no special DES mass flow controller available. A correction of the automatic N₂ mass flow controller for DES is necessary.

At the beginning, the volume of the CVD chamber was determined by flowing a known amount of N₂ into the CVD chamber with initial pressure and boost valve was closed for 10min. The initial pressure and the final pressure after 10min were measured and the ideal gas law, $PV = nRT$, was used to calculate the volume of the reactor.

Suppose the N₂ in the CVD chamber is an ideal gas, the volume of the CVD chamber can be read:

$$V = \frac{760 * (FR) * t * T}{273 (P_{fN} - P_{iN})} * 10^{-3} \quad (17)$$

where FR is the flow rate of N₂ in SCCM ; t is the time in min , T is the temperature in the chamber in K, P_{iN} and P_{fN} are the pressures of the N₂ in torr initially and finally , respectively; and V is the volume of the CVD chamber in liters.

The results are in *Table 2*. The volume of the CVD chamber is taken as 17.87 liter. We assume the temperature, T, in the chamber to be 298K.

FR (SCCM)	t (min)	P _{iN} (torr)	P _{fN} (torr)	V (liter)
51	10	0	23.8	17,76
100	10	0	46.5	17,81
150	10	0	69.2	17.95
200	10	0	92.0	18.00
250	10	0	116.1	17.84
Average Value				17.87

Table 2. Data for the determination of the volume of the CVD chamber.

By using the CVD chamber volume, the real flow rate of DES can be determined conveniently in a similar way. The factor for DES is defined as the ratio of the real flow rate of DES to the "N₂" flow rate in the mass flow controller.

DES vapor flowed into the CVD chamber and was controlled by the N₂ mass flow controller. The initial pressure in the chamber and the pressure after some time flow are read using the pressure gauge.

Suppose the vapor of DES is an ideal gas, the real flow rate of DES, FR(R), and the factor for DES can be obtained, respectively:

$$FR(R) = \frac{17.87 * (P_{fc} - P_{ic})}{760 * t} \frac{273}{T} * 10^3 \quad (18)$$

$$\text{Factor} = \frac{FR(R)}{FR} \quad (19)$$

where FR(R) and FR are the real flow rate of DES and flow rate of N₂ in SCCM; P_{ic} and P_{fc} are the pressure of DES in the CVD chamber initially and finally; t is the time in min and T is the temperature in the chamber. 17.87(l) is the volume of the chamber.

The experimental results are listed in table3. In the range of the flow rate in this study, the factor for DES is assumed to be 0.19.

FR (SCCM)	Time (min)	P _{ic} (torr)	P _{fc}	FR(R) (SCCM)	Factor
294	5	0	13.3	57.4	0.195
294	10	0	26.9	58.0	0.197
59	10	0	5.2	11.2	0.190

Table 3. Factor for DES in N₂ mass flow controller.

2.2 The procedures in this CVD study

Experiments at different vapor flow rates, DES pressures and temperatures have been performed. The depositions were carried out at temperatures between 600 and 850C at

constant pressure 0.2 torr and flow rate 30SCCM; pressures between 0.05 and 0.30 torr with a constant temperature 700C and flow rate 30SCCM; and at flow rates between 10 and 50 SCCM with a constant pressure 0.2 torr and temperature 700C.

The deposition rate values were derived from layer mass on both sides divided by CVD time, in units of mg/hr.

The thickness of the films deposited on the wafers was measured with a Nanospec interferometer. During this study, the index of refraction could not be obtained accurately so that the index of refraction was taken as 2.8. This results in some instrumental error in the measurement of the thickness. As expressed by Fig.4, five points were taken in the measurement of the thickness. The radial variations in the thickness over the wafer were defined as follows:

$$\text{Variation}[\pm] = 100 * (d_{\max} - d_{\min}) / (d_{\max} + d_{\min}) \quad (6)$$

with d_{\min} and d_{\max} being the minimum and maximum film thickness measured in the wafer center and 10 mm from the wafer edge.

The chemical compositions of the produced films arose from the measurement of RBS on the films. The film's morphology was determined by an x-ray diffraction. The bonding and hydrogen content were obtained by IR spectroscopy.

The etch characteristics of the films in KOH solution were determined by watching the microstructures and measuring the wafer's mass before and after the etching to 0.1 milligrams. The etching solution of KOH is 22.5% in wt% concentration and 70C in temperature. The etching time is 15min.

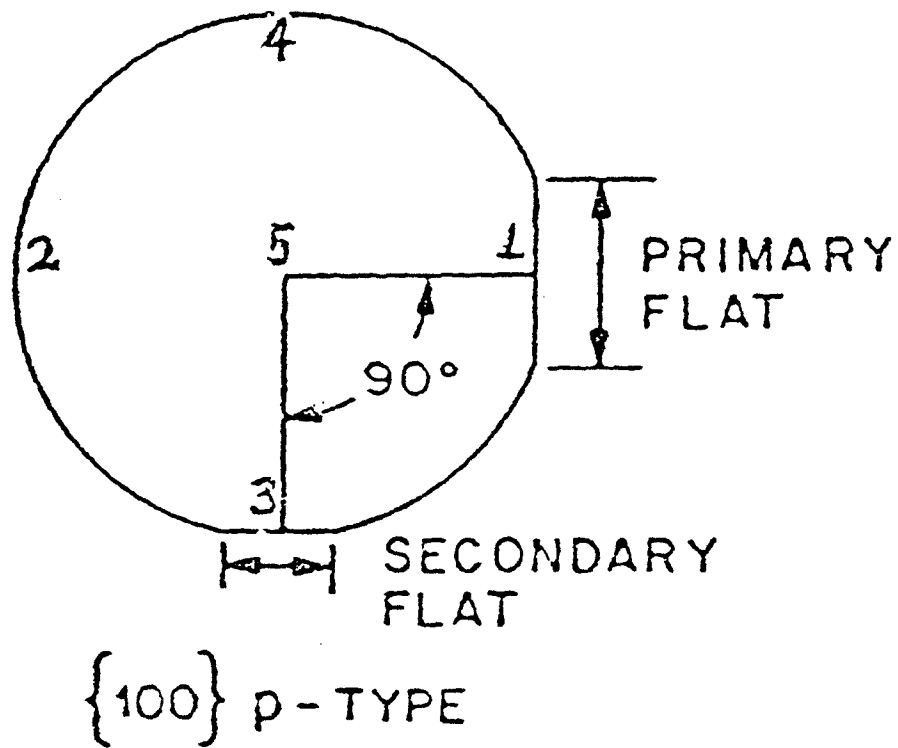


Fig.4 Identifying flat on a (100) Silicon wafer. The thickness of the films were measured at point 1, 2, 3, 4, and 5.

3. RESULTS AND DISCUSSION

3.1 Kinetics and gas flow in the CVD

In this study, the average deposition rate on the six wafers, $D.R.$, has been used for characterizing deposition rate for a well defined CVD condition in order to correct the depletion effects. $D.R.(z)$ ($z = 1, \dots, 6$) is defined as the deposition rate at z -th wafer. The degree of relative deposition rate along the length direction, $D.R.(z)/D.R.(1)$, shows the depletion effects. The less the value of $D.R.(z)/D.R.(1)$, the stronger the depletion effects.

3.1.1. Temperature and Activation energy

In Fig.5, the temperature dependence of deposition rate can be seen. At low temperature, the deposition rate follows an exponential law: $D.R. \sim \exp(-E_a / RT)$. The activation energy E_a is about 41 Kcal/mol. At higher temperature, the deposition rate is almost independent of temperature. Since chemical reactions generally follow an exponential temperature dependence while the mass transfer process is independent of temperature, region A in Fig.5 is characterized as surface reaction-controlled and region B in Fig.5 is characterized as mass transfer-controlled. The connection point at this CVD conditions ($P = 0.2$ torr, flow rate = 30 SCCM) is about 725C.

The relationship between $D.R.(z)/D.R.(1)$ and z ($z = 1, \dots, 6$) at different temperatures displays the depletion effects of temperature. At higher temperature, the CVD process shows stronger depletion effects, as seen in the axial thickness variation (Fig.6), with distance along the reactor, than that at lower temperature. This can be explained by the fact that less reactive gas is available in the following wafer because of more rapid consumption of DES at high temperature than that at low temperature.

3.1.2. Gas flow and kinetics

The degree in relative deposition rate along the length direction, $D.R.(z)/D.R.(1)$, at different pressures, is plotted in Fig.7 where it is seen that the axial deposition rate

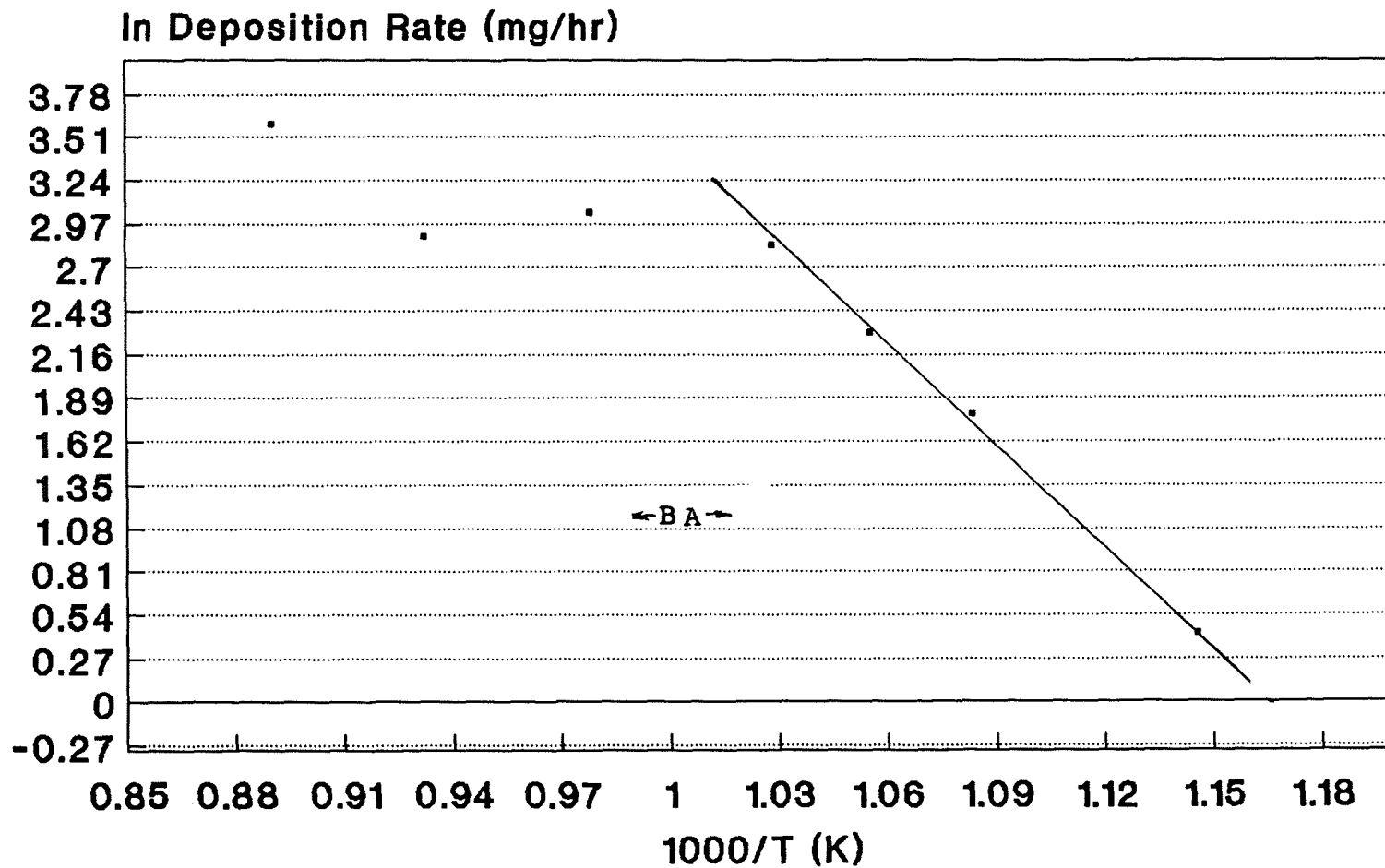


**Fig.5 The temperature dependence
of deposition rate
Pressure is 0.2torr, Flow rate is 30SCCM**

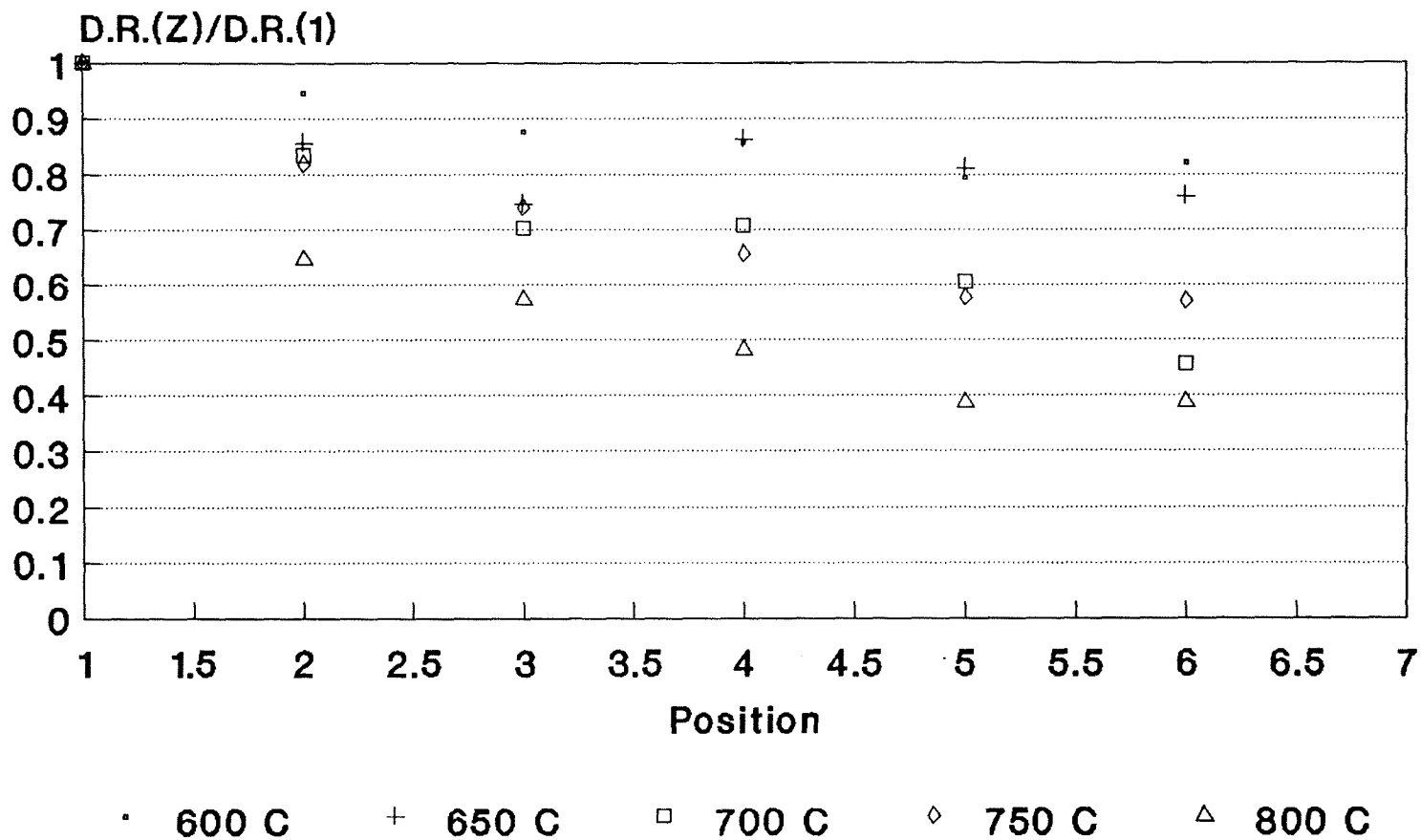
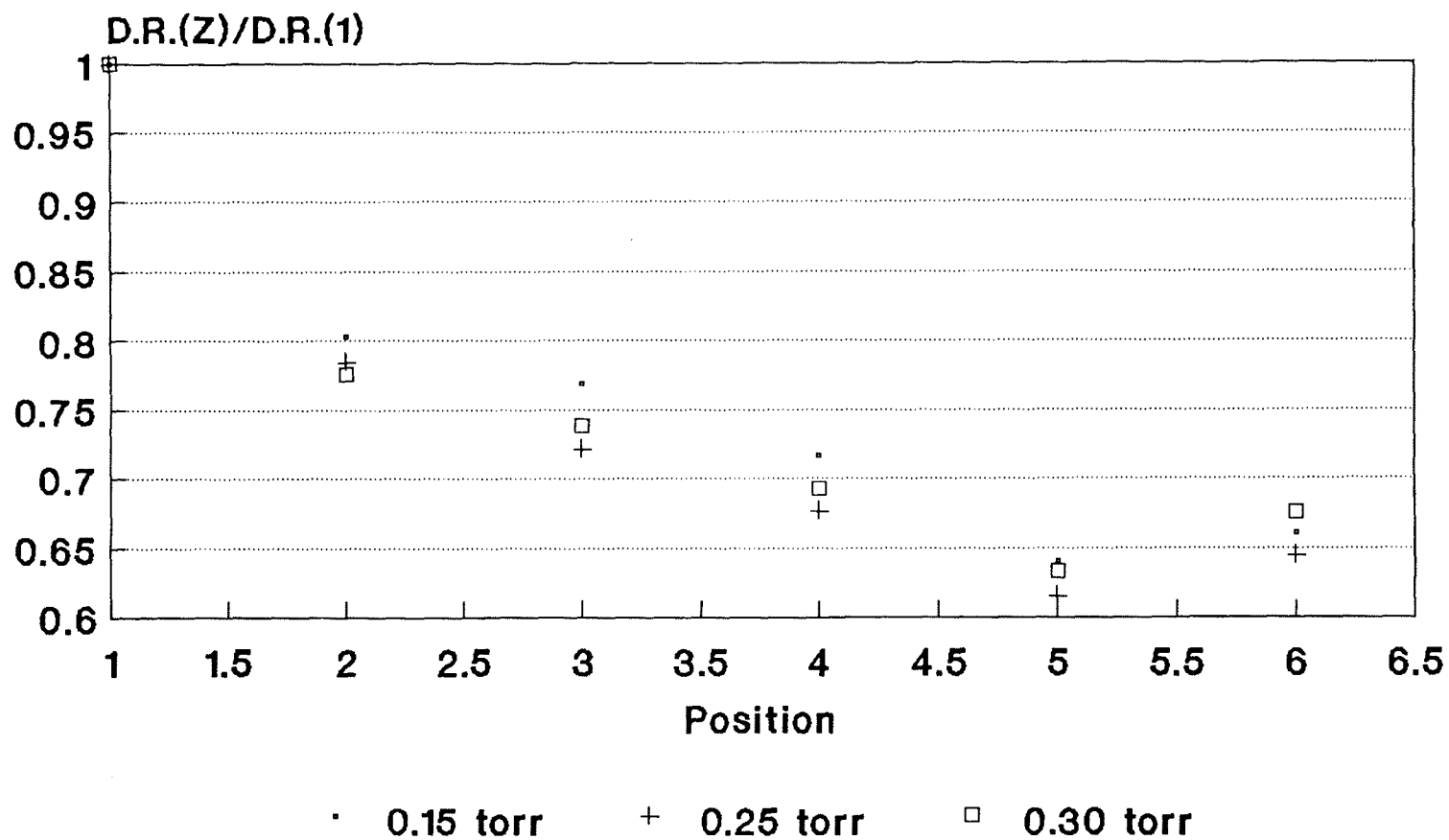


Fig.6. Normalized deposition rate versus position in the reactor for DES Pressure is 0.2 torr, Flow rate is 30 SCCM



**Fig.7. Normalized deposition rate
versus position in the reactor for DES
Temperature is 700C, Flow rate is 30SCCM**

decrease diminishes upon DES pressure increase. The axial deposition rate variation is also dependent on the gas flow velocity (Fig.8). At the low gas velocity(u) in the annular part (i.e.,the space between the row of the wafers and the tube wall) a strong depletion in deposition rate is found. An increase in gas flow rate results in a flattening of the deposition rate profile.

It should be noted that the depletion effect has stronger dependence on the CVD reactor temperature than the pressure and the flow rate in the ranges investigated, as expressed by Figures 6, 7 and 8.

When deposition rate values are plotted versus the gas flow rate with the pressure 0.2torr and temperature 700C it is found, as shown in Fig9, that this deposition rate varies strongly at low gas flow rates, and a saturation effect is observed at large gas flow. These results show that the deposition rate depends on the flow conditions.

The shape of the curves in Fig.9 therefore reflects the increase in the steady - state DES concentration in the gas phase with increasing flow velocity. This increase is the result of the competition between supply of DES by the input gas flow and consumption of DES at the substrate surface. This means that only the deposition rate at high gas flow is limited by flow dynamics effects.

In Fig.10, deposition rate values are plotted versus the pressure of DES. It is seen that for a CVD condition, i.e. constant flow rate and reactor temperature, a less than linear dependence is found. In fact , the shape of the curve suggests that the deposition rate is limited by an adsorption mechanism, as will be discussed in the next section.

The combined occurrence of both a decrease in the axial deposition rate(Fig.7) and the sudden increase of radial inhomogeneity in layer thickness at the input pressure of DES roughly above 0.05torr, shows that the mass transport process can not be described merely by gas phase diffusion and heterogeneous decomposition of DES.

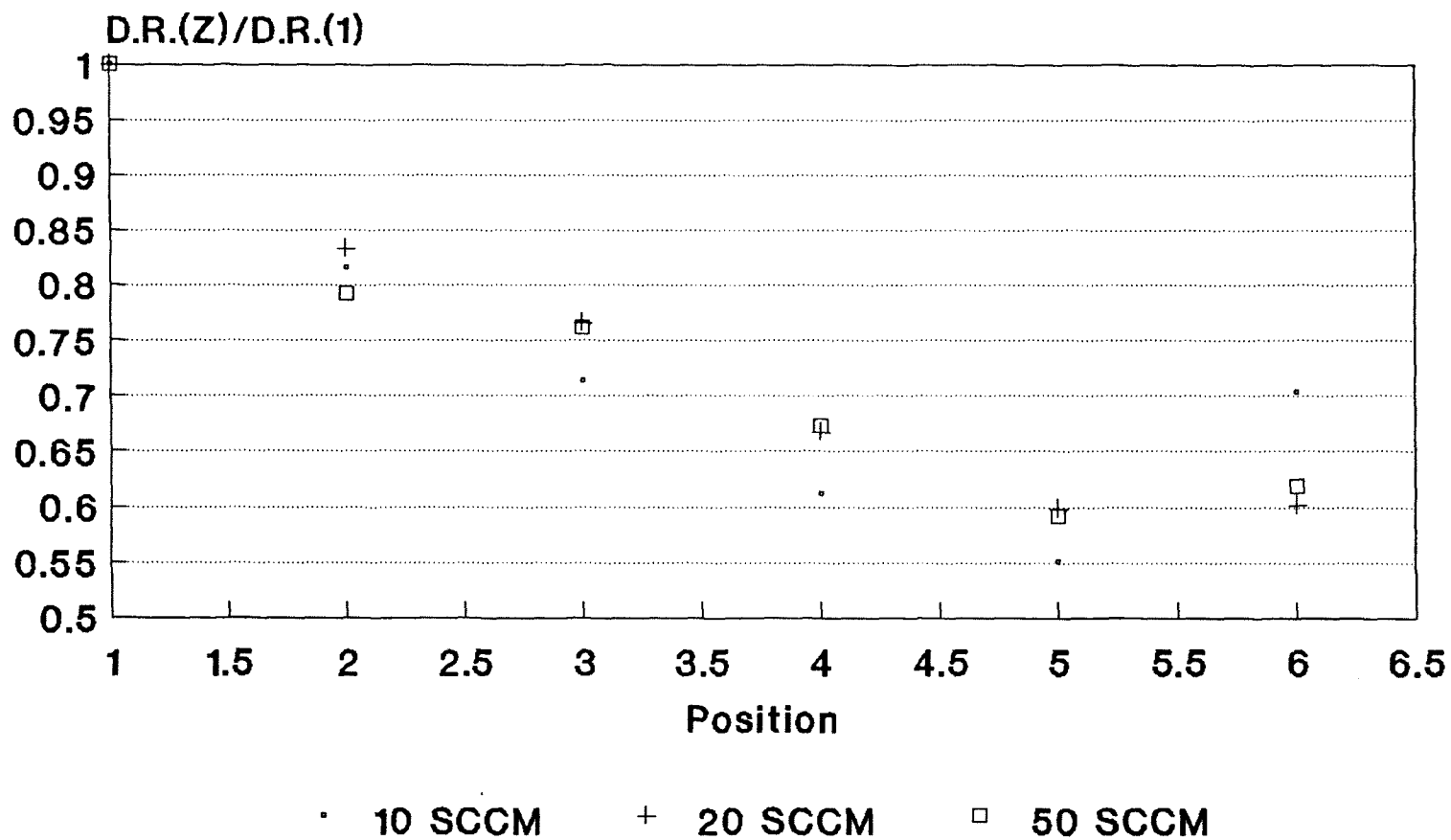


**Fig.8. Normalized deposition rate
versus position in the reactor for DES
Pressure is 0.2torr, Temperature is 700C**

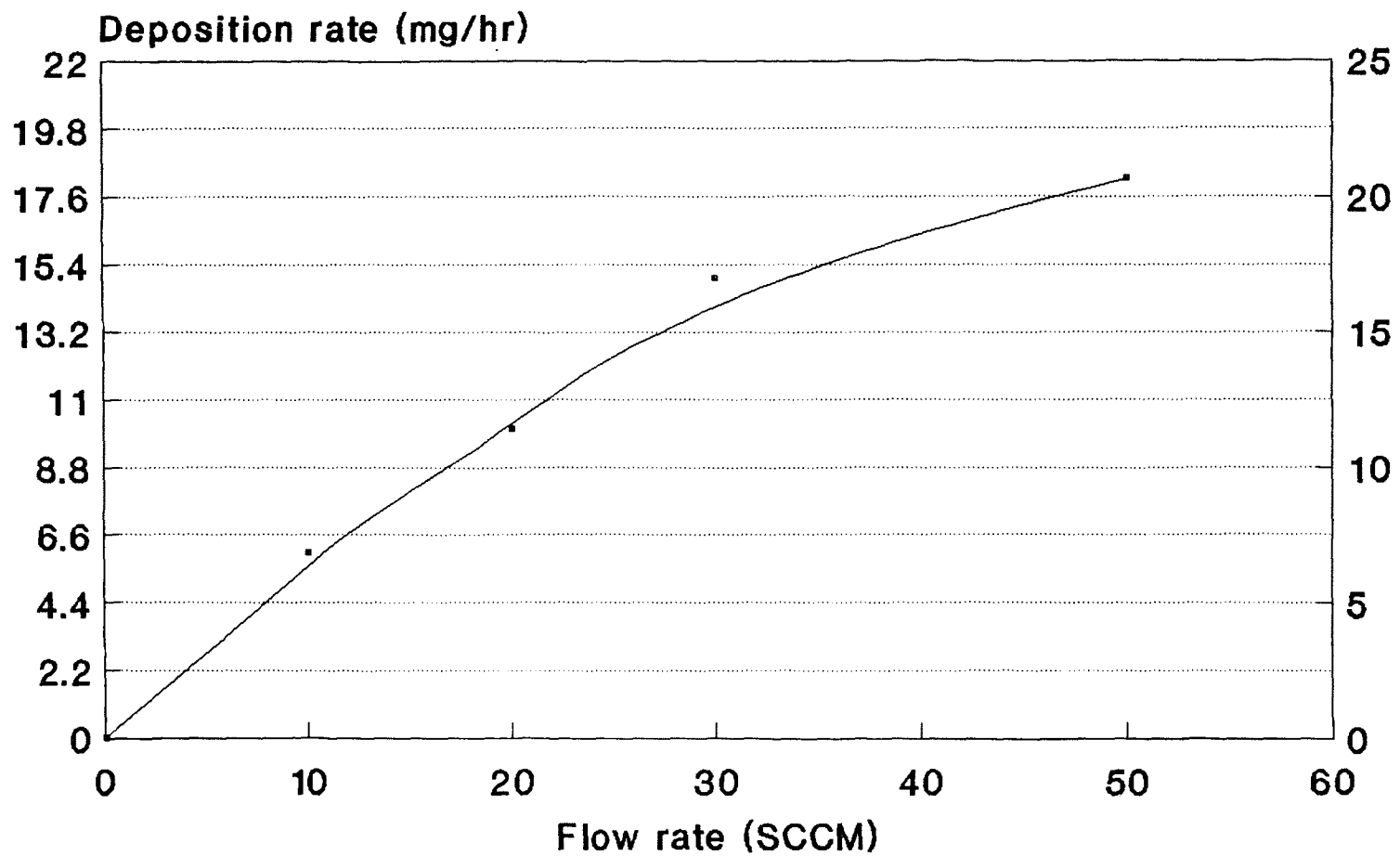


**Fig.9 The relationship between
deposition rate and flow rate.
Temperature is 700C, Pressure is 0.2torr**

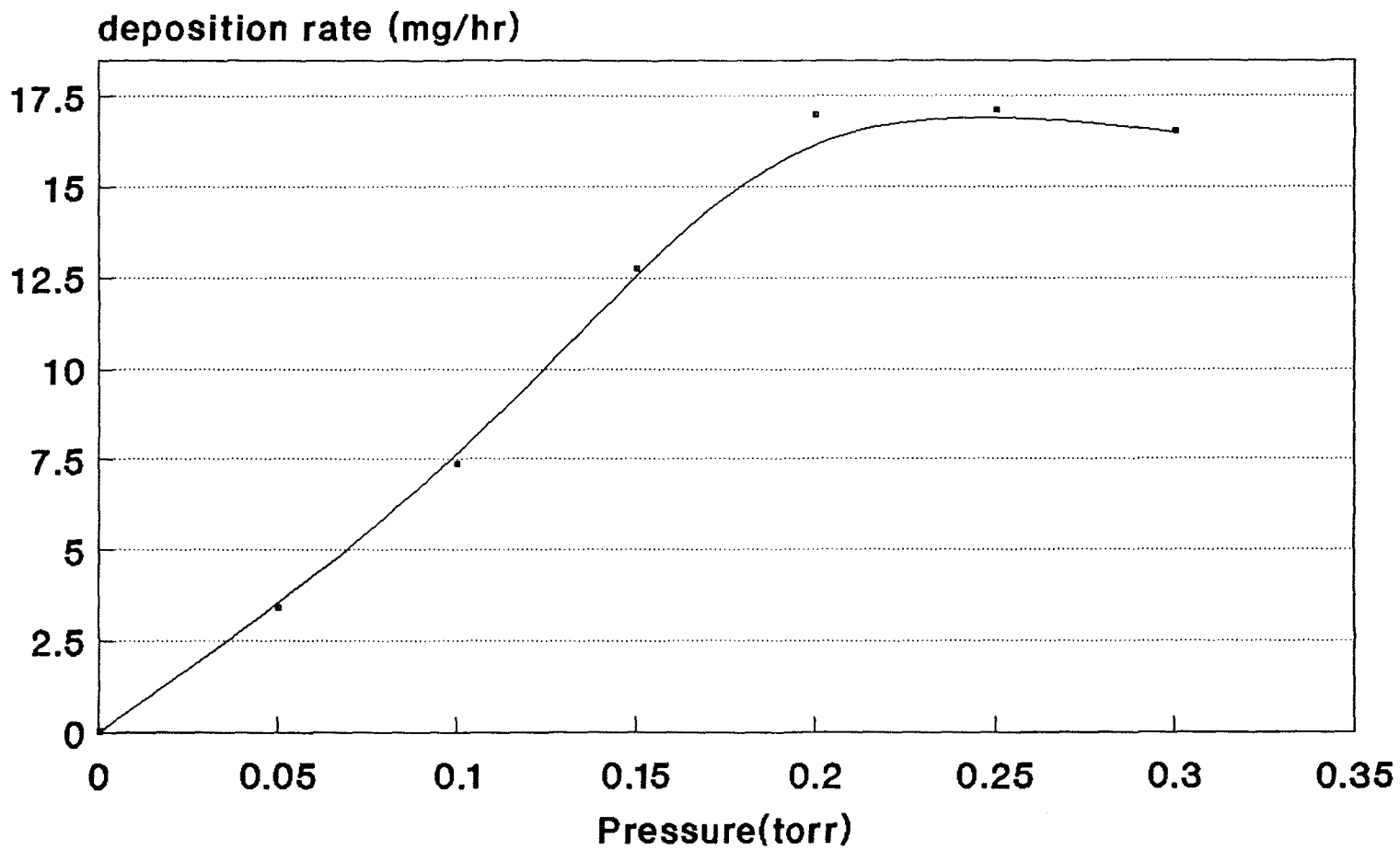


Fig.10 The relationship between the pressure and deposition rate. Temperature is 700C, Flow rate is 30SCCM

3.1.2.1 Low input DES pressure

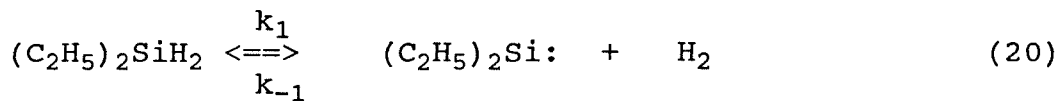
The deposition process at relatively low DES input pressure is extremely surface-controlled(27). The measured deposition rate values therefore provide the information about the reaction mechanism. The data of Fig.10 clearly shows the non-linear relationship for the deposition rate. At very low pressure a strong dependence of the deposition rate on the input pressure is observed, whereas for higher values of the pressure a saturation of the deposition rate is found.

The relationship, which has been obtained from deposition rate values, now explains why the decrease in axial deposition rate (see Fig.7) depends on the absolute value of the input pressure. The local slope of such a curve(Fig10), which depends on the applied pressure, thus introduces a strong variation in axial deposition rate at low pressures but a small variation in deposition rate at high pressures.

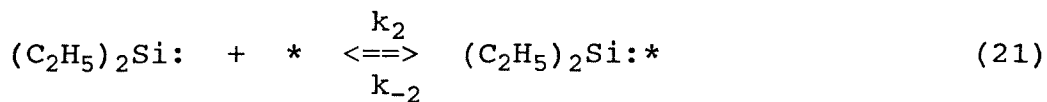
3.1.2.2. Reaction mechanism

Dialkylsilanes begin to decompose at 440-460C through homolytic cleavage of the Si-H bond and subsequent radical formation(31,29). Furthermore, an adsorption mechanism is considered as a limitation for the deposition rate. Being similar to SiH₄(11,12), the following gas phase and surface reactions are taken into account:

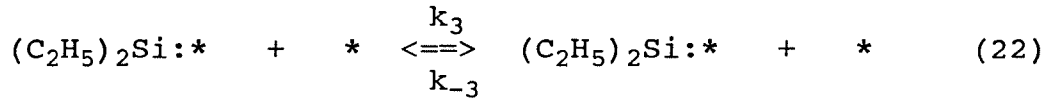
(a) Gas phase dissociation



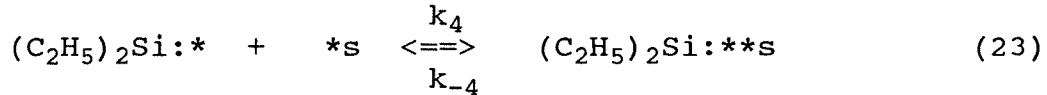
(b) Adsorption on a free surface site, denoted by *



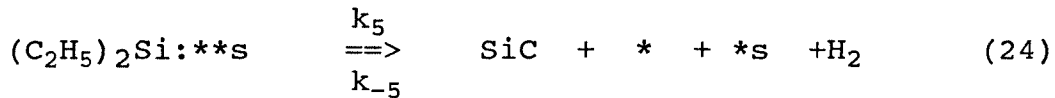
(c) Surface diffusion:



(d) Incorporation of silicon at a free step site or a kink position, denoted by *s:



(e) Release of hydrogen:



The fraction of free surface sites on the substrate surface (θ) and at steps (θ_s) can be defined as

$$\theta = 1 - \theta_{(C_2H_5)_2Si:} \quad , \quad \theta_s = 1 - \theta_{s,:(C_2H_5)_2Si} \quad (25)$$

where $\theta_{(C_2H_5)_2Si:}$ is the fraction of sites occupied by adsorbed $(C_2H_5)_2Si:$ molecules.

In this case, $(C_2H_5)_2Si:$ is the most important silicon-carbon containing compound on the substrate and the adsorption of atomic hydrogen, which has not been found in the IR spectroscopy described below, can be neglected in the range of temperatures used in this study.

According to the experimental data, the rate-limiting step has to be found in one of the surface reactions(b) to (e). The following additional conclusions are useful in determining the rate-limiting step:

(i) If adsorption were rate-limiting, k_2 would be much smaller than k_{-2} , leading to a large fraction of free surface sites almost equal to unity. According to the experimental data in Fig.10, the deposition rate saturates as the DES input pressure increases. These experimental data can only be explained by the availability of a small fraction of free sites. Site availability is strongly dependent on the DES pressure. The adsorption of $(C_2H_5)_2Si$: is thus not expected to be rate-limiting.

(ii) Surface diffusion can not be rate-limiting because surface diffusion can be excluded in amorphous growth.

(iii) Discrimination between the reactions(d) and (e) as being rate-limiting is difficult. However, it is assumed that k_5 is rate-limiting because the temperature dependence of k_5 has the same sign as the apparent activation energy of the deposition rate.

These three points lead to the conclusion that k_5 , the release of hydrogen, is rate-limiting. In this case it may be assumed that the previous reactions are in equilibrium and the deposition rate can be given as

$$D.R. = k_5 \theta_{S, Si(C_2H_5)_2} = k_5 K_4 K_2 \theta \theta_S p_{Si(C_2H_5)_2} \quad (26)$$

In order to find the relation between $p_{Si(C_2H_5)_2}$ and the input pressure of DES $p^0(C_2H_5)_2SiH_2$, it is convenient to introduce the decomposition parameter α :

$$\begin{aligned} p_{(C_2H_5)_2SiH_2} &= (1-\alpha) p^0(C_2H_5)_2SiH_2 \\ p_{Si(C_2H_5)_2} &= \alpha p^0(C_2H_5)_2SiH_2 \end{aligned} \quad (27)$$

with eq.(21) the fraction of $(C_2H_5)_2Si$: molecules adsorbed on the silicon surface is given by $\theta_{(C_2H_5)_2Si} = K_2 P_{(C_2H_5)_2Si} \theta$. With $\theta = 1 - \theta_{Si(C_2H_5)_2}$ (eq.(25)) and eq.(27), we obtain:

$$\theta = (1 + K_2 \alpha P^0_{(C_2H_5)_2SiH_2})^{-1} \quad (28)$$

For θ_s we can find an almost identical expression

$$\theta_s = (1 + K_2 K_4 \theta \alpha P^0_{(C_2H_5)_2SiH_2})^{-1} \quad (29)$$

combining eqs. (28) and (29) leads to

$$\theta \theta_s = (1 + K_2 \alpha P^0_{(C_2H_5)_2SiH_2} + K_2 K_4 \alpha P^0_{(C_2H_5)_2SiH_2})^{-1} \quad (30)$$

The deposition rate, as given by eq.(26), can now be replaced by

$$D.R. = k_5 K_4 K_2 \alpha P^0_{(C_2H_5)_2SiH_2} [1 + \alpha K_2 P^0_{(C_2H_5)_2SiH_2} (1 + K_4)]^{-1} \quad (31)$$

An expression for α can be found by inserting the expression given by eq.(27) in eq.(20).

With $K_1 = k_1/k_{-1}$, this give us:

$$\alpha = K_1 / (K_1 + P_{H_2}) \quad (32)$$

K_1 is large with respect to p_{H_2} , making $\alpha = 1$

From this we may conclude that for low pressure deposition conditions, eq.(31) can be simplified into

$$\text{D.R.} = \frac{a P^0 (\text{C}_2\text{H}_5)_2\text{SiH}_2}{1 + bP^0 (\text{C}_2\text{H}_5)_2\text{SiH}_2} \quad (33)$$

where a and b are constants. This expression is quantitatively in agreement with the experimental findings (Fig.10).

The less than linear dependence of the deposition rate upon the DES pressure (eq.31) is effective in reducing axial and radial thickness variation. In the case of high input concentration, possible differences in the local concentration of diethylsilene, due to slight diffusion limitations, will result in smaller deposition rate differences than for the linear case. In fact the mass transfer coefficient, as used in the definition of the Sherwood number, is proportional to the local slope of the curve where the deposition rate is plotted versus the input pressure on a linear scale (to be constructed from Fig.10). Consequently, the tendency of the curve to saturate should decrease the radial thickness variation. From Fig.11, at the pressure range from 0.15 torr to 0.3torr, the relationship meets the above rule. However, when the pressure changes from 0.05 torr to 0.15 torr, the appearance of a more obvious inhomogeneous layer can not be explained by the tendency of the curve (Fig.10) to saturate. This behavior must be attributed to an additional effect, which becomes dominant at a range of low input concentration. The homogeneous gas phase polymerization is also found to be responsible for this effect.

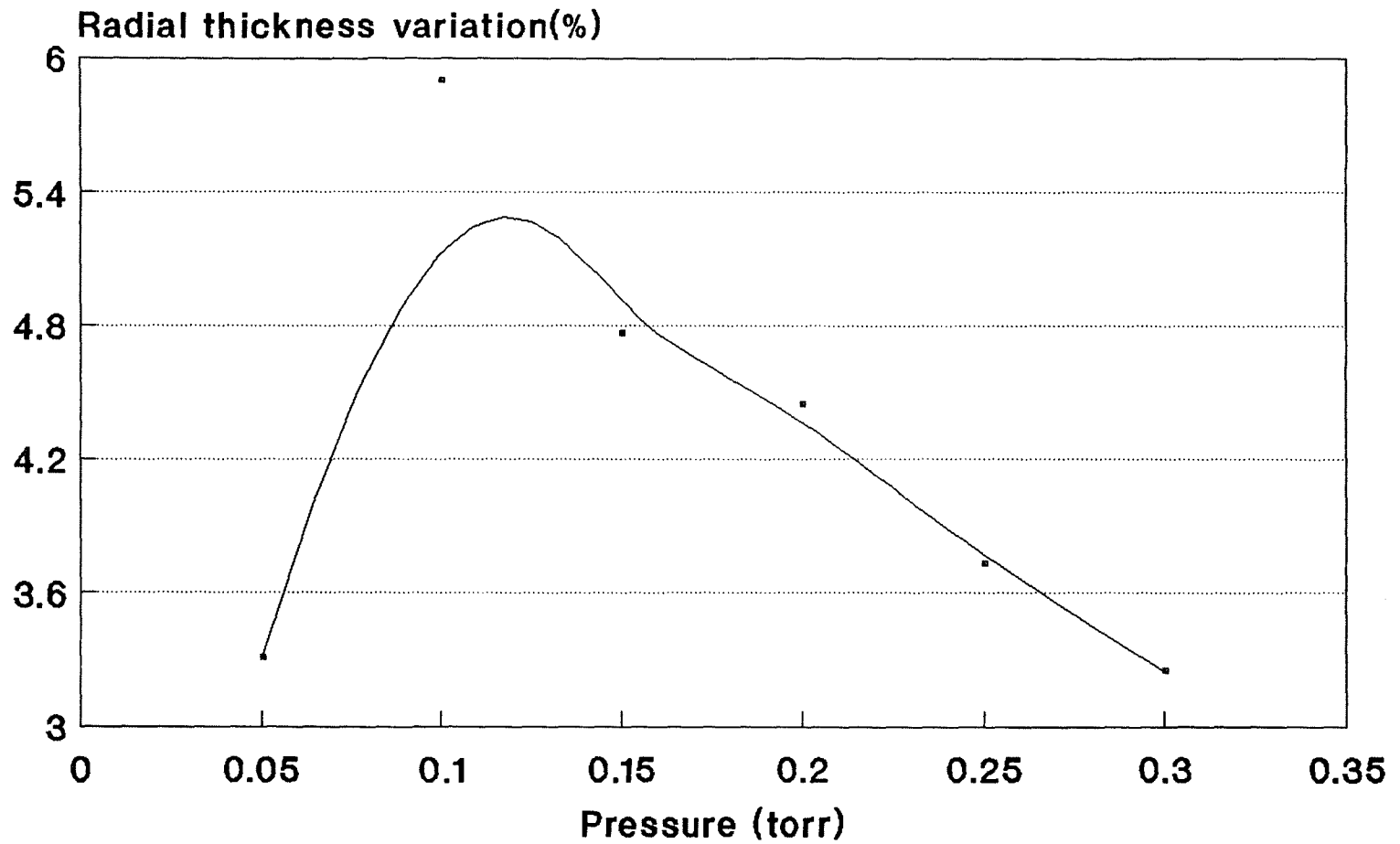
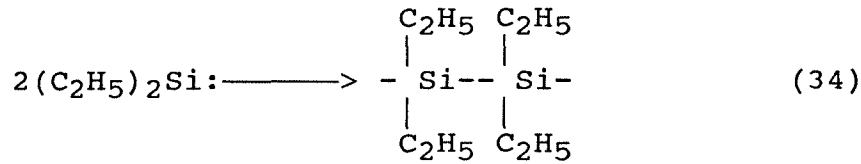


**Fig.11 The relationship between radial thickness variation and pressure
Temperature is 700C, Flow rate is 30SCCM**

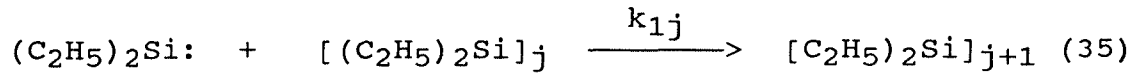
3.2. Polymerization and its deposition

3.2.1. Homogeneous gas phase polymerization

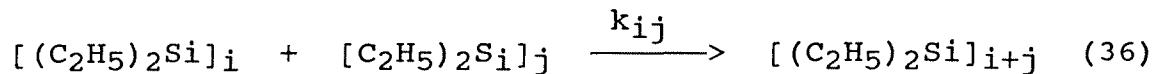
The homogeneous decomposition of DES is supposed to have the similar mechanism for the dimerization process with silane(29) and the overall reaction reads:



based on the same principle , we now propose further polymerization reactions in which diethylsilene reacts with a j-mer, $[(\text{C}_2\text{H}_5)_2\text{Si}]_j$:



as well as the combination of two polymers



The number of collisions between molecules i and j per unit time according to the kinetic gas theory is given by:

$$N_{ij} = n_i n_j \sigma_{ij}^2 \left(\frac{2\pi kT}{m_i m_j} \right)^{1/2} , \quad (37)$$

where n_i is the number of molecules of type i per unit volume, $\sigma_{ij} = 1/2 (d_i + d_j)$ is the effective collisions surface, d_i is the diameter of molecules of type i , k is Boltzmann's constant, T is the gas temperature and, m_i is the mass of molecules of type i .

The kinetics of polymerization during the time-of-flight of DES in the hot zone can be described mainly on the basis of reaction(35), since excess diethylsilene is available. The production rate of polymers is then given by

$$\frac{dn_{i+1}}{dt} = \zeta N_{1i}, \quad (38)$$

where ζ is the effective probability factor for reaction (35), assumed to be independent of i to a first approximation. For very low pressure of DES, n_1 will be small and so will N_{11} , N_{12} , N_{13} , ... N_{1i} , which means that polymerization remains negligible. The degree of polymerization will, however, rapidly increase when the initial DES pressure approaches some critical pressure, which is strongly dependent on the temperature. High n_1 values promote the formation of higher polymers. It will be clear that the larger the polymer molecules the more impacts of silylene will occur, due to an increased σ_{1i} . In particular reactions as given in (36) then become important and enhance the polymerization. This model shows that this mechanism, which is operative above the critical DES pressure, leads to an avalanche-like production of high polymers.

3.2.2 Deposition with the polymer

At relatively high pressure, the gas phase does not exclusively contain monodiethylsilane but contains some distribution of polymers. This means that under such conditions, apart

from the diffusion of $(C_2H_5)_2Si$, the transport of each polymer kind must also be taken into account.

The diffusion coefficient of an i-mer in the gas phase, D_{iO} , is given by

$$D_{iO} = \frac{3}{8\pi n_O \sigma_{iO}^2} \left(\frac{kT (m_i + m_O)}{2\pi m_i m_O} \right)^{1/2} \quad (39)$$

It should further be recognized that the deposition of an i-mer results in the deposition of i silicon atoms, which means that the mass transfer coefficient, k_{Di} also depends on i and to a first approximation

$$k_{Di} = i k_{D1} \quad (40)$$

Since the diffusivity decreases and k_{Di} increases with increasing i, the Sherwood number, Sh_i , of the deposition process of i-mers approximately increase:

$$Sh_i / Sh_1 = i^{5/3} \quad (41)$$

Because homogeneous coverage in CVD processes is only possible when the Sherwood number is small enough, the presence of heavy polymers in the gas phase will necessarily result in inhomogeneous deposits, while at the same deposition temperature, pressure and substrate arrangement, the monomers will yield a homogeneous coverage. The ultimate shape of the radial thickness profile in LPCVD will be the results of the superposition of the action of all i-mers present in the gas phase. This model satisfactorily explains that the radial deposition rate variations increase rapidly when the initial DES pressure increases from 0.05 torr to 0.15 torr.

In the other range of pressure, 0.15-0.30 torr, the effect of polymerization, which decreases the diffusivity, is greater than that at lower pressure. However, the opposite effect, the tendency of the deposition rate as a function of pressure to saturate, should make the radial thickness variation decrease because the mass transfer coefficient, K_D , is proportional to the local slope of the curve (deposition rate vs pressure). In this pressure range, the saturation of deposition rate as a function of pressure becomes dominant, so the total results are a drop in the Sherwood number and a decrease in the radial thickness variation of the film with increased pressure.

Besides pressure, the deposition temperature is also a very important influence on the polymerization in the deposition process. With increasing temperature, the degree of polymerization is raised rapidly so that the diffusivity decreases and the mass transfer coefficient increases with increasing i , resulting in an increase of the Sherwood number, Sh_i (in eq. (41)). The increase of temperature has two results: first, the surface reaction is faster; secondly, the Sherwood number of the deposition process of i -mer approximately increases. These two effects result in the process becoming diffusion limited and tending towards a homogeneous reaction at high temperature.

As discussed above, the degree of polymerization will rapidly increase when the initial DES pressure approaches some critical pressure, which is strongly dependent on the temperature. The critical DES pressure can be roughly estimated by the aid of Fig.11. The curve from 0.05 torr to 0.12 torr shows a nearly constant local slope, from which we would conclude that at 700C, strong polymerization occurs at least from 0.05 torr. On the other hand, Fig.12 indicates that at 0.2torr pressure, strong polymerization happens when the temperature is above 700C. The two observations indicate the rough relationship between the critical pressure of DES and the deposition temperature, that is, the critical pressure decreases very rapidly with the increase of temperature.

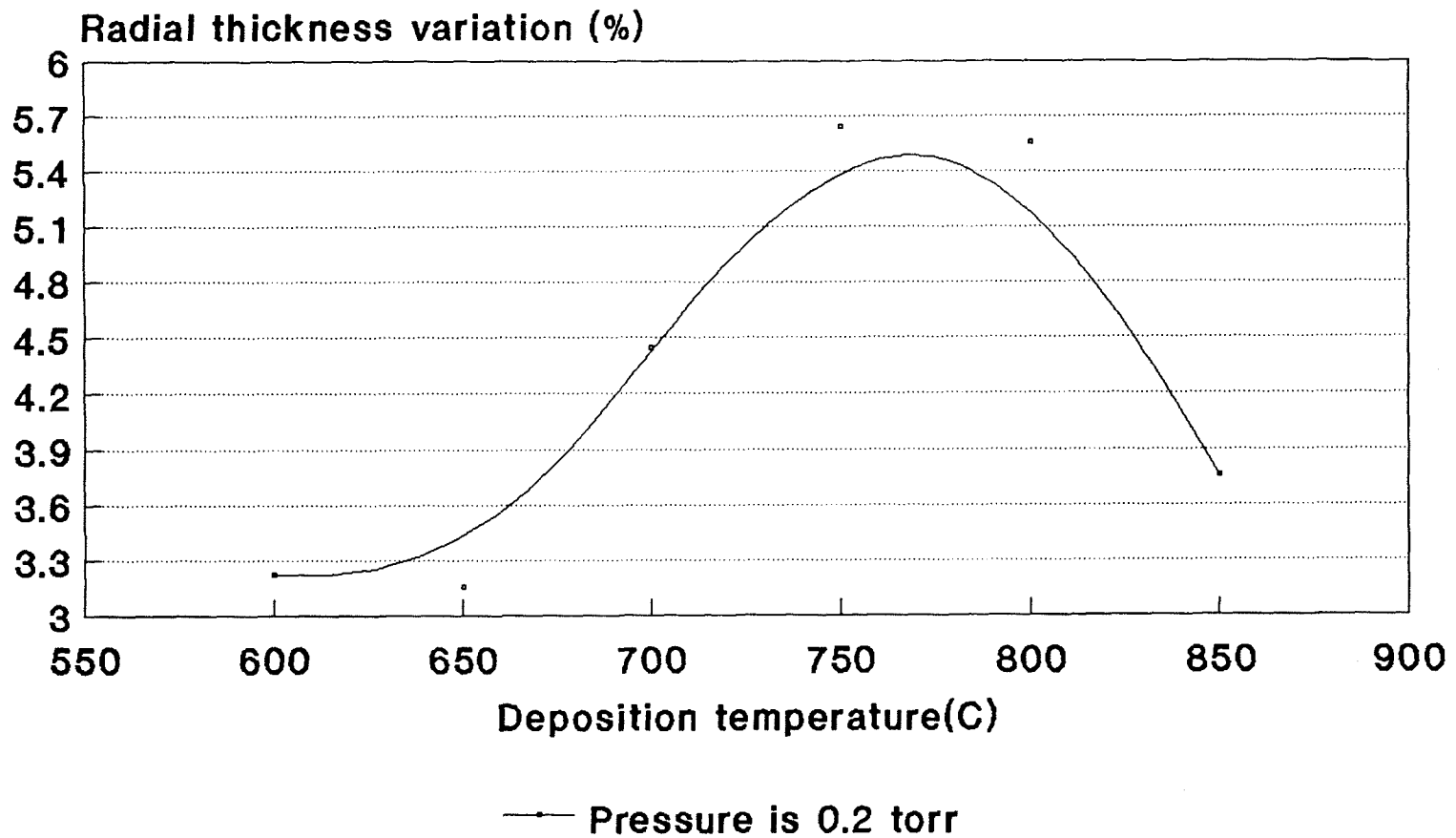


Fig.12 The relationship between radial thickness variation and deposition temperature

It should be noticed that the curve in Fig.12 shows an interesting decrease in radial thickness variation when the temperature is above 780C. As will be detailed later, an X-ray diffraction peak corresponding to β - SiC crystal was observed for a deposition temperature of 850C, that is, the film contains β - SiC. For this deposition, the surface diffusion is important. The process suggests that the surface diffusion becomes stronger and stronger so that the radial thickness variation decreases with increasing temperature. Deposition at 780C, at which the radial thickness variation begins to decrease, can be considered as the point at which the adatom begins to diffuse and organize into order so that the density of the film is obviously raised as shown in the appendix, in which the densities of the films deposited at different conditions have been listed. The films deposited at temperatures higher than 800C possess denser films than at the lower temperature.

In addition, the homogeneous polymerization also results in the deviation of the kinetic characteristics from the typical kinetic equations of a completely heterogeneous process in some degree even if Fig.5 and Fig.10 indicate a heterogeneous mechanism in the CVD process. For example, although the deposition rate is almost independent of temperature as was expressed in Fig.5, some decrease in deposition rate can be observed with the increase of temperature at the temperature range of 800-850C, in which the homogeneous polymerization is suggested.

3.3.Film Evaluation

3.3.1. RBS, X-Ray and IR Spectroscopy

In general, the chemical composition of a film is a function of temperature, pressure, flow rate and source gas composition in an LPCVD system. In this study, the chemical composition as a function of temperature, pressure, or flow rate when the other independent variables are constant have been investigated by RBS and shown in Fig.13,14

and 15. The film deposited at a temperature of 600C, a pressure of 0.2 torr and a flow rate of 30 sccm is stoichiometrical, and the other films are Si-rich at different degrees. All of the films reveal typical spectra of transmittance(%) versus wave number(cm^{-1}) for silicon carbide thin film in spite of the low energy effect resulting from B-Si substrate absorption in measurement. However, the peak corresponding to the Si-H bonding at 2600 cm^{-1} has not been found, which indicates that the hydrogen content in the films can be ignored. The IR spectrum is given in Fig.16. X-ray diffraction studies, which are shown in Fig.17, have a typical (111) plane diffraction peak of β -SiC when the deposition temperature is 850C or above. Those show us that the films are amorphous materials at temperatures lower than 850C, or β -SiC crystal at temperatures of 850 or above.

3.3.2. Optical Microscopic Examination

The ideal film should be smooth, contain no cracks, have no gas phase nucleation and possess no other defects. Microstructures observed by an optical microscope indicate the qualities of the films. In this study, the films produced at low temperature, low pressure or low flow rate show better microscopical smoothness and less gas phase nucleation than those produced at higher temperatures, higher pressures or higher flow rates. These results coincide with the conclusion that the strong polymerization is formed at high temperature or high pressure. Secondly, most films have expansive cracks if the thickness of the film is above 0.6-0.7 μm . The dependence of the cracks strongly suggests that these cracks mainly result from the 20% mismatch in the coefficients of thermal expansion according to Fatemi and Nordquist (32). Thirdly, there are some point defects on some films. The microstructures of the thin films are expressed in Fig.18.

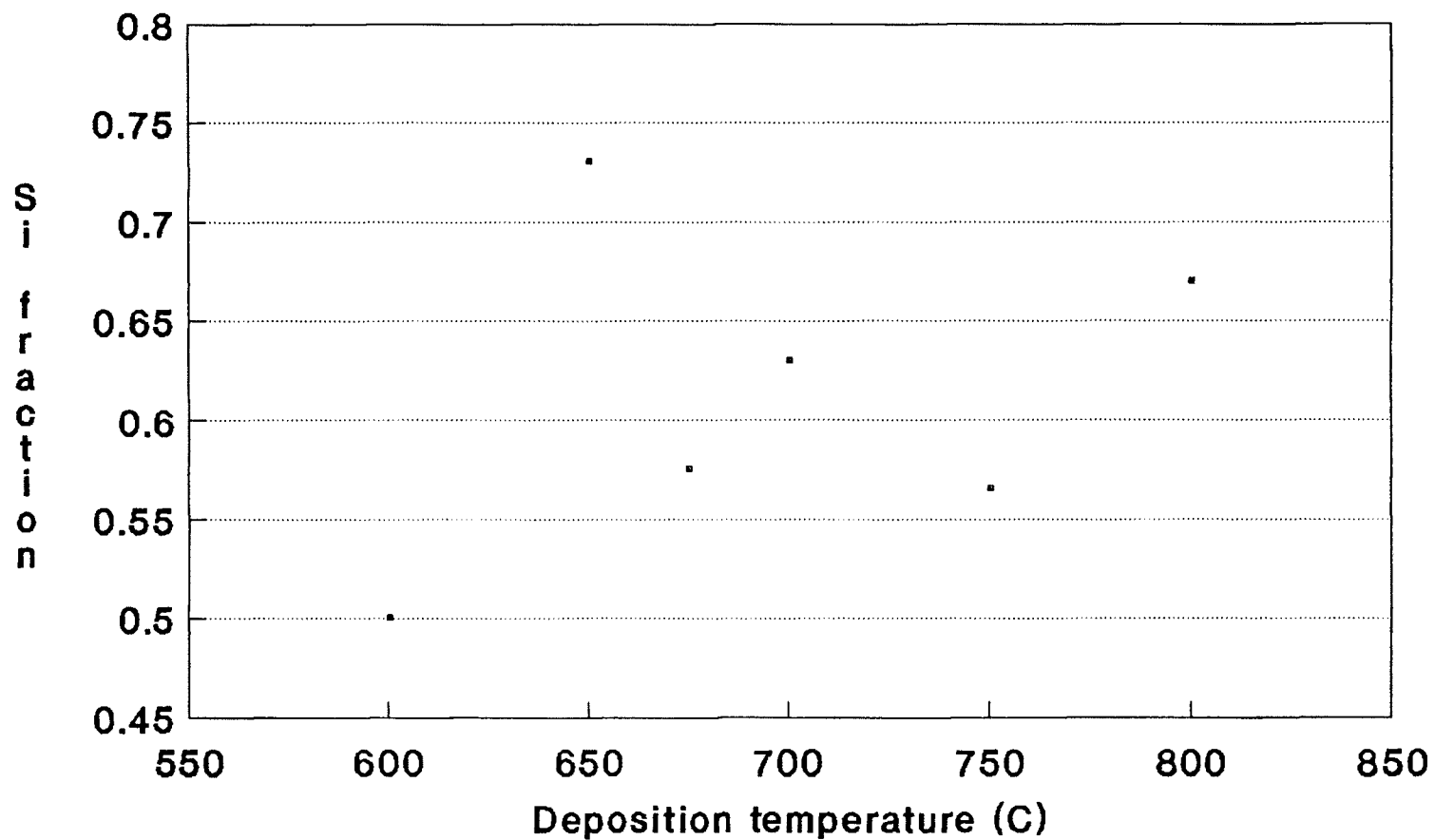
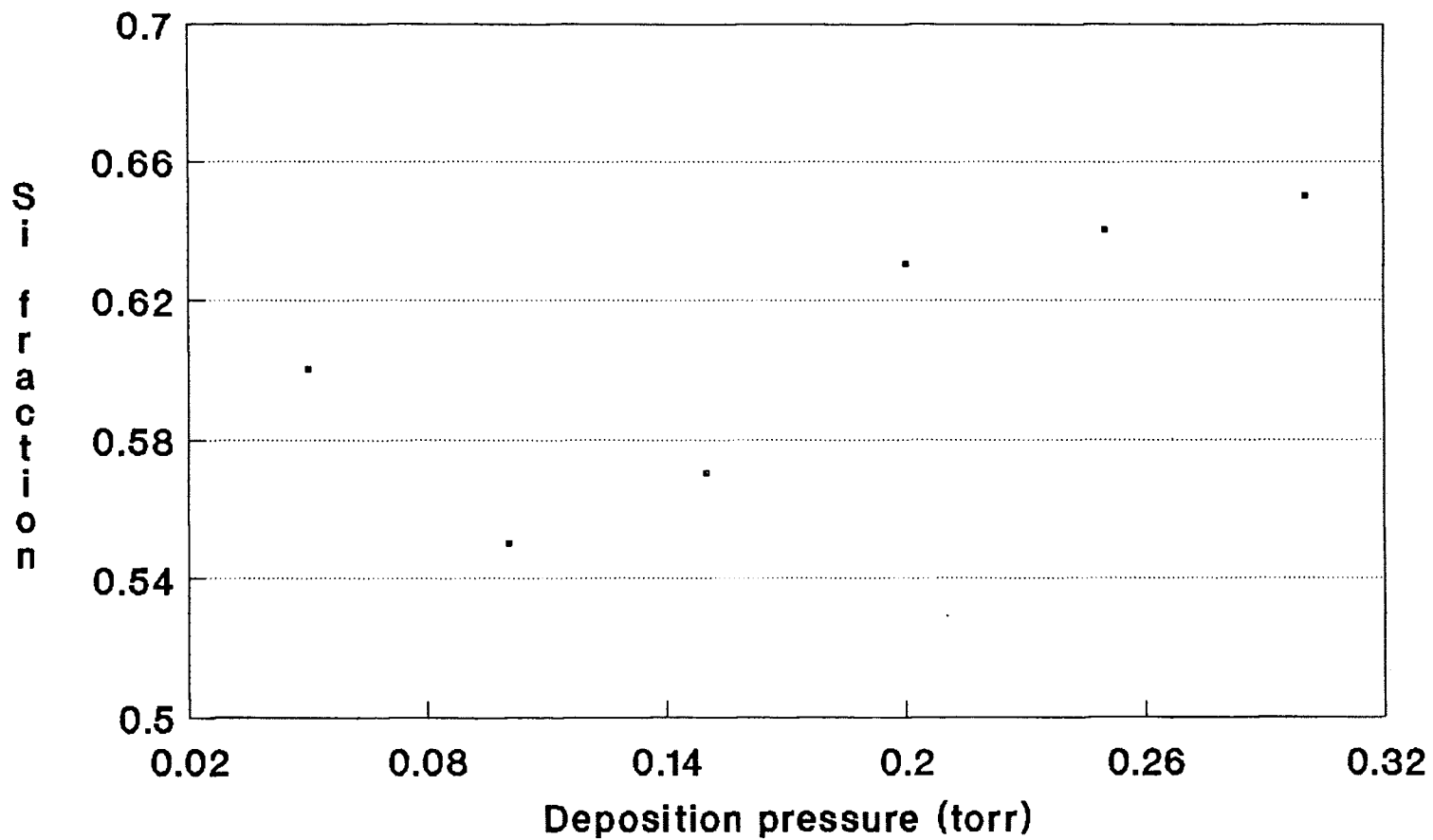
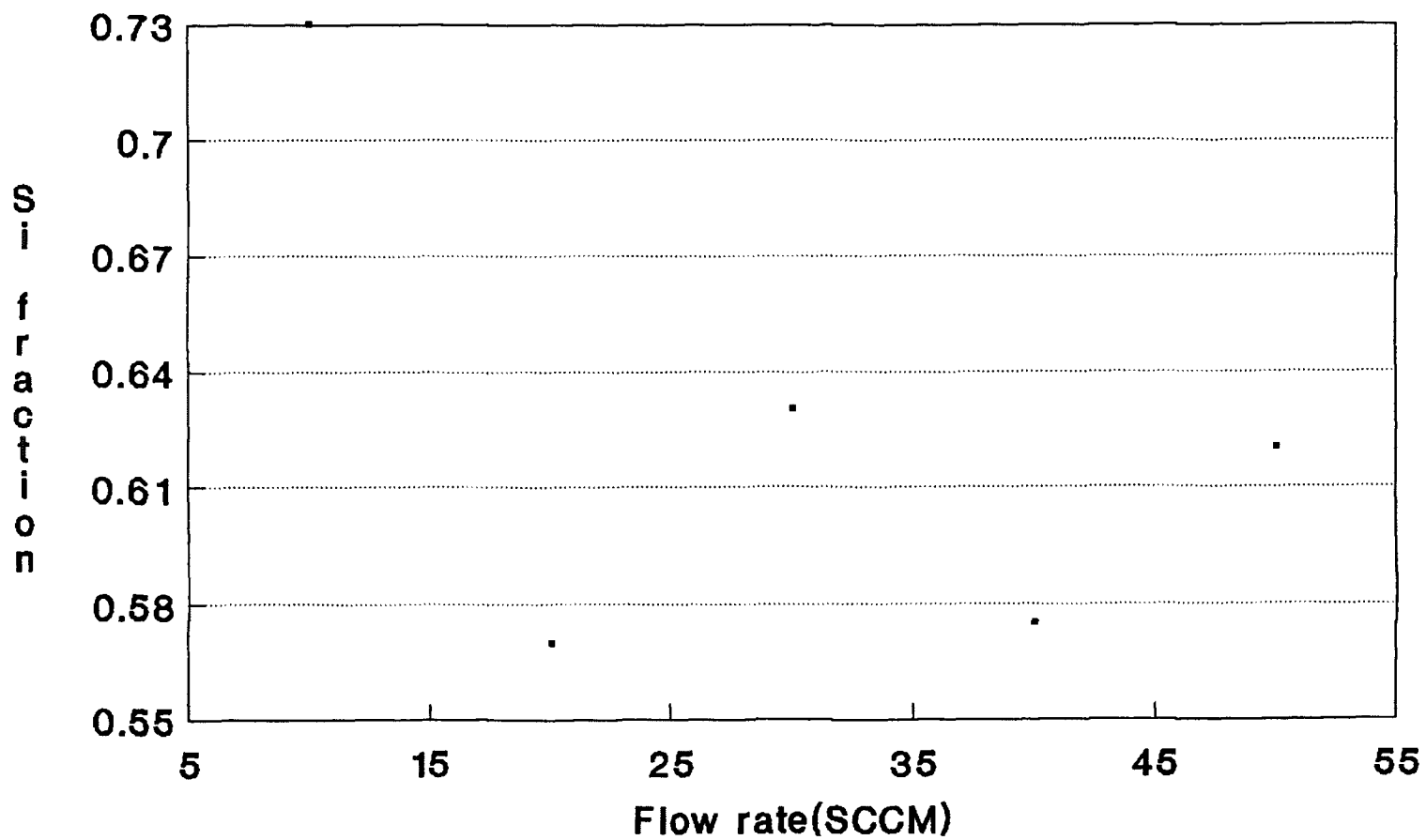


Fig13 The relationship between chemical composition and deposition temperature. Flow rate is 30SCCM, Pressure is 0.2torr



**Fig14 The relationship between chemical composition and pressure.
Flow rate is 30SCCM, Temperature is 700C**



**Fig15 The relationship between chemical composition and flow rate.
Pressure is 0.2torr, Temperature is 700C**

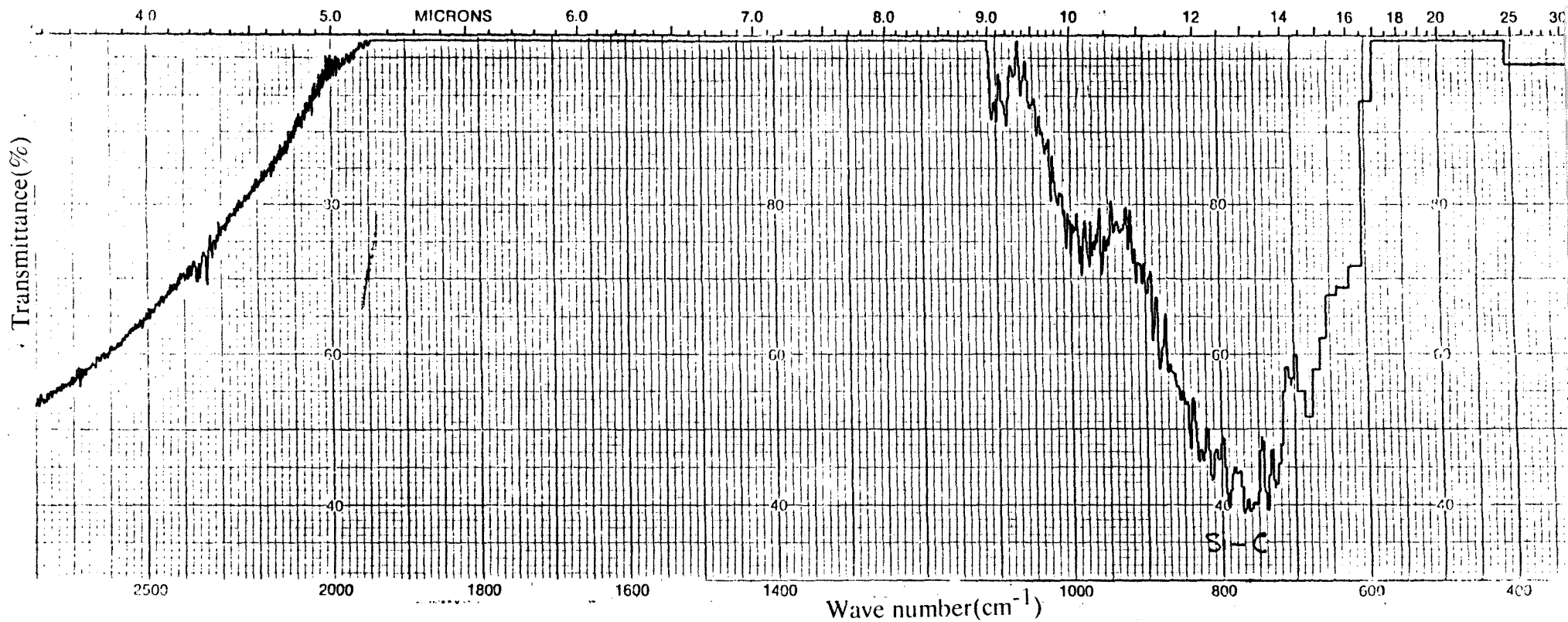


Fig.16. IR spectroscopy of the films
 A typical spectrum of transmittance(%) versus wave number(cm-1) for silicon carbide thin films is illustrated. In this study, all of the films possess almost the same IR spectra

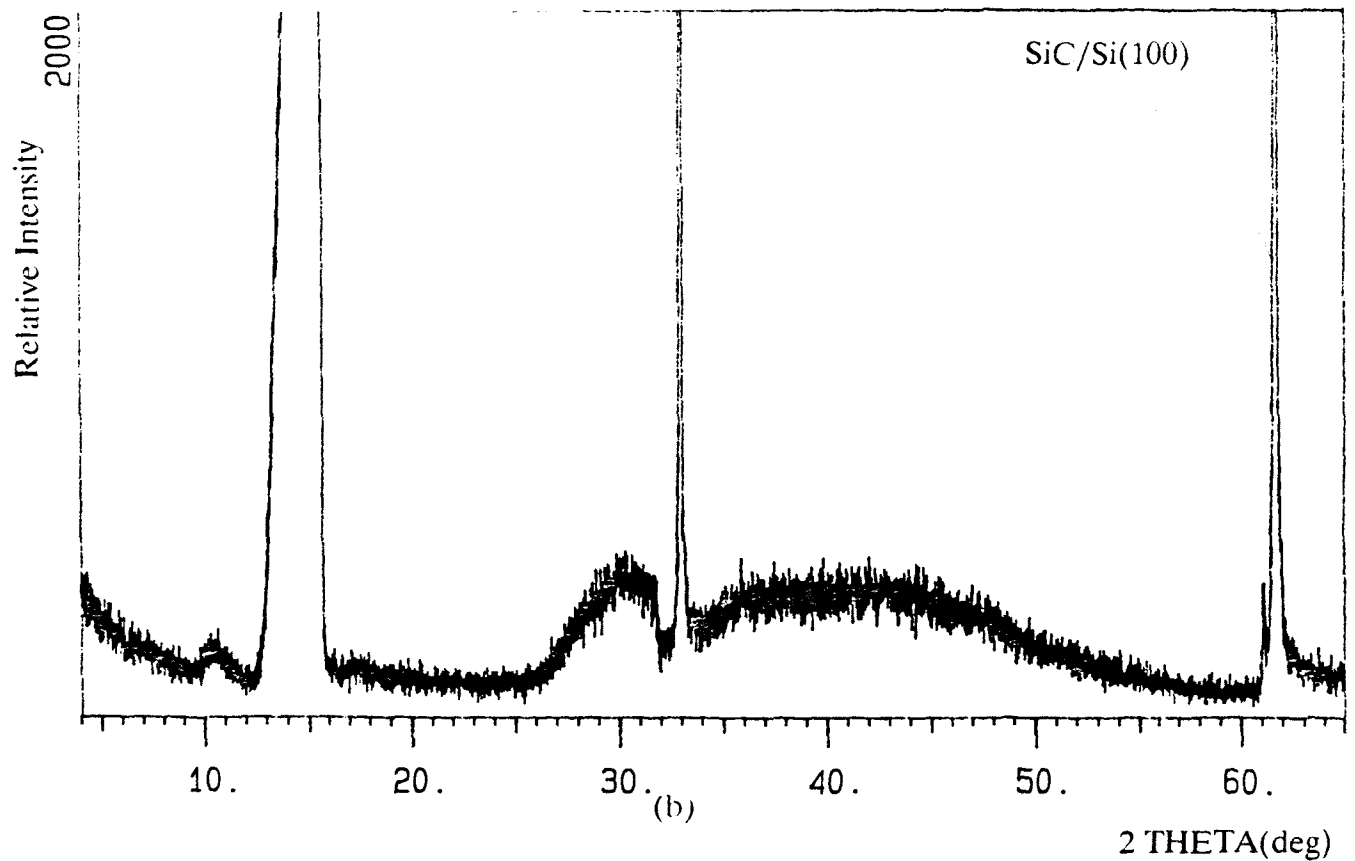
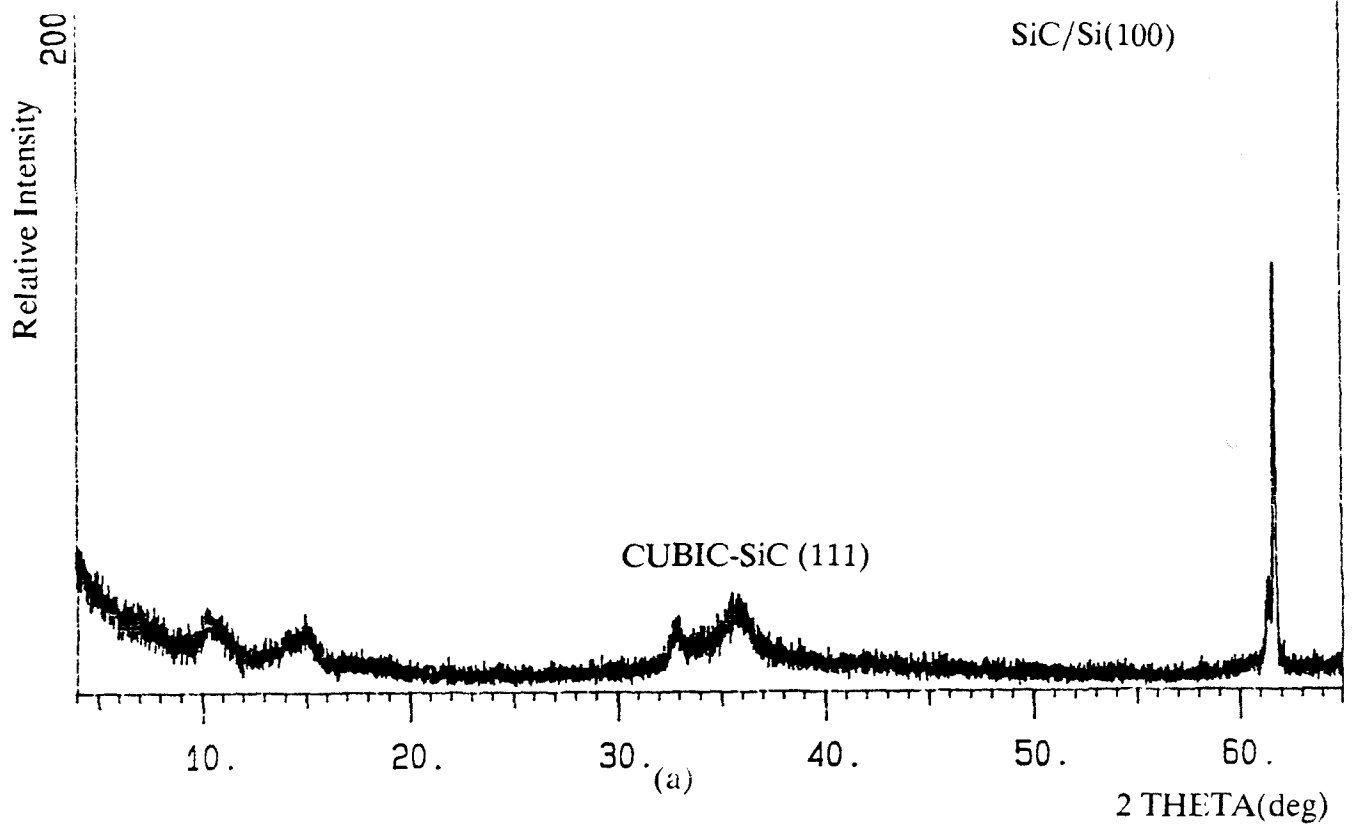
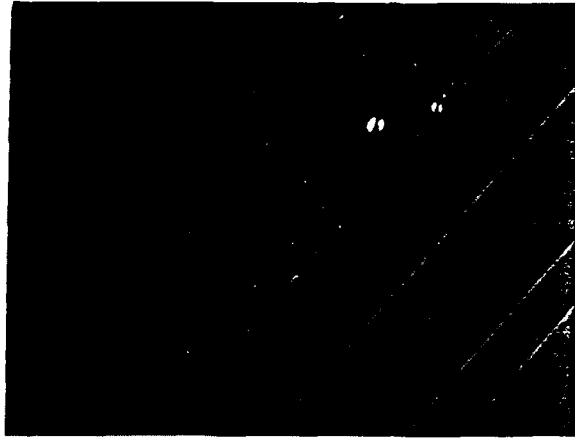
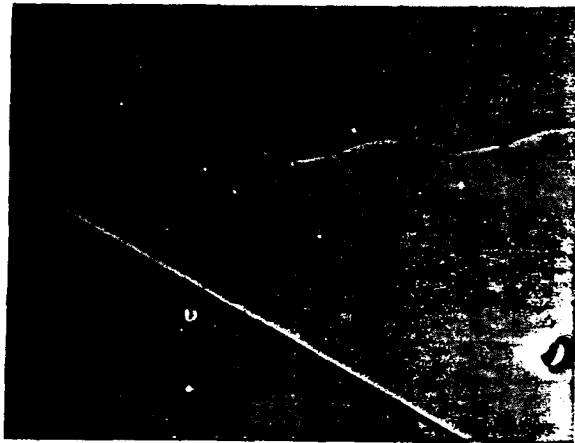


Fig.17. X-ray diffraction patterns. There is a marked difference between the two X-ray diffraction patterns. The curve (a) for the SiC film deposited at 850C shows (111) cubic-SiC peak, while the curve (b) for the SiC film deposited at 800C shows only Si substrate peaks.

650C°



700C°



800C°

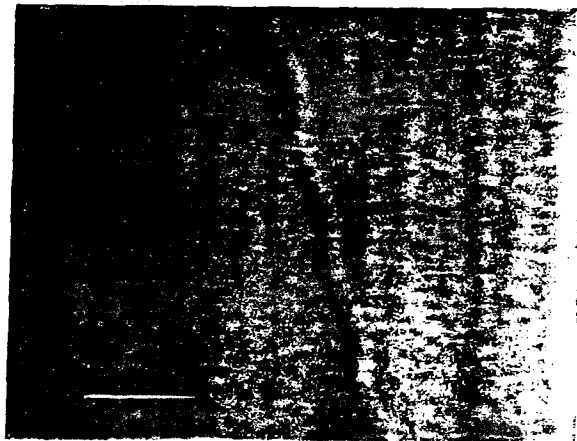
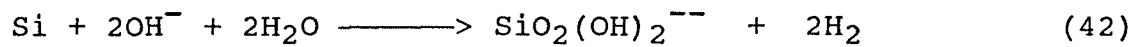


Fig.18: Microstructures of thin film surfaces. The films from top to bottom were deposited at 650C, 700C and 800C. The film produced at low temperature shows better microscopical smoothness and less gas phase nucleation than those at higher temperature. The amplification is 110 x.

3.4 Etching Study

In the present research, the author made the etching study of amorphous SiC in KOH solution. As is known, monocrystalline SiC does not react with KOH solution. However, the Si substrates react with the etching solution:



The driving force for this reaction is given by the large Si-O bonding energy of 193Kcal/mol as compared to a Si-Si bonding energy of only 78Kcal/mol.

In this study, when the wafers with the amorphous SiC films are put into the KOH solution, the defects of the films were expanded, and small point defects can be observed after etching. Thus, the etch pit density in the films and the size and density of the cracks expanded by etching have been taken as Evaluation Indexes of the films. Since some of the films peeled off from the substrates after deposition and the effect of peeling off will be enhanced by etching, the mass of the films peeled off from the substrate in etching has also been used as an Evaluation Index for the evaluation of the films. The smaller the mass, the better the films.

The films produced have the etching characteristics that the cracks expanded in their length and width direction, some point defects were observed and some of the films peeled off from the substrates after the 15 min etching. However, the degrees are different. If the Evaluation Indices are used, the film's quality can be arranged in order. Table 4 shows the orders of the size and density of the defects, the mass of the film peeled off from the substrate in etching, the Si fraction of the films, the thickness of the films, and the temperature in CVD reactor, where Y8, Y16, Y4, ... are the wafer ID number. From the table, the conclusions are as follows:

(a). The film's ability to prevent etching has an obvious relationship with Si fraction in the film. The lower the Si fraction in the films, the more difficult the etching.

(b). There is no relationship between the thickness and the ability for the film to prevent etching, Nor is there a relationship between the etching ability of the film and the temperature or pressure in CVD reactor.

(c). The more the Si fraction in the film, the more the mass of the film peeled off from the substrate in etching. In other words, the adhesion power of the film decreases with the increase of Si fraction in etching.

Fig.19 shows the microscopic observations of the films after the 15-minute etching.

As a hypothesis, the author proposes that the silicon in amorphous SiC films (including Si-rich and C-rich films) can react with KOH:H₂O etching solution according to the chemical reaction equation (42), but the carbon can not react with the etching solution. As a result, the etching characteristics are a function of Si fraction of the films and the KOH:H₂O etching results in porous films in which the porosity depends upon the Si fraction. This hypothesis shows why the pits can be observed, the films are peeled off by the etching and the etching results have the obvious relationship with Si fraction in Si-rich films. However, although most of the films used in the etching study have a Si fraction greater than 0.5, as described in Section 3.3, the film with Si fraction of 0.5 is also etched according to the comparison between the microscopic observations before and after etching (the surface became rough after the 15-min etching), which means the experimental results and the hypothesis are not limited to Si-rich films. Furthermore, another experiment indicated that the etching rate of amorphous C-rich films can be ignored. According to the hypothesis, the less Si-fraction in C-rich film results in a much lower reaction with the films and the much denser Carbon-Surface-Layer formed by etching prevents further.

Series ID	Comparison
Deposition temperature	Y16 < Y8 < Y4 < Y30 < Y33
Thickness of films	Y16 < Y8 < Y33 < Y30 < Y4
Si fraction	Y16 < Y30 < Y4 < Y33 < Y8
The quality according to the defects produced by etching	Y16 > Y30 = Y4 > Y33 > Y8
The difference of masses between before etching and after etching $\left(\frac{w_B - w_A}{w_B} \times 100\% \right)$	Y16 < Y4 < Y30 < Y33 < Y8

Table 4. Etching study in temperature series wafers in which the deposition temperature changed but the input pressure and the flow rate are constant. Y16, Y8, etc. are the wafer ID number, and "<" and ">" mean less than and more than, respectively.

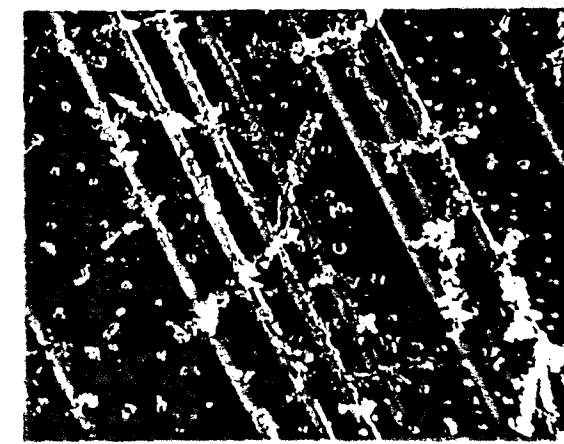
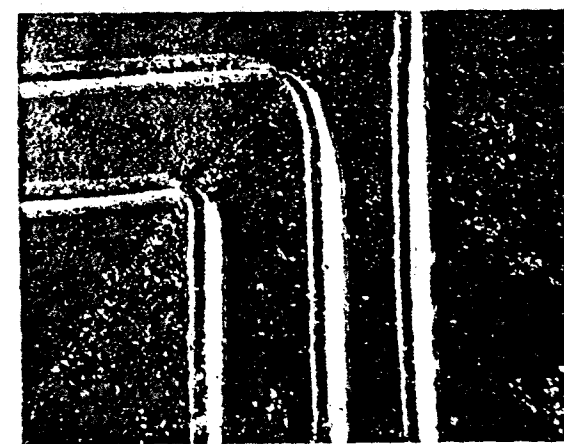
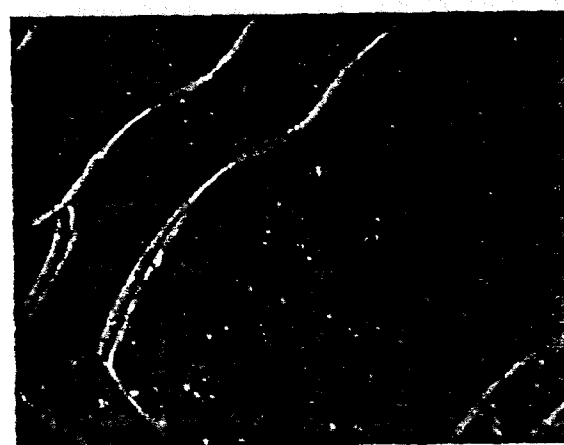
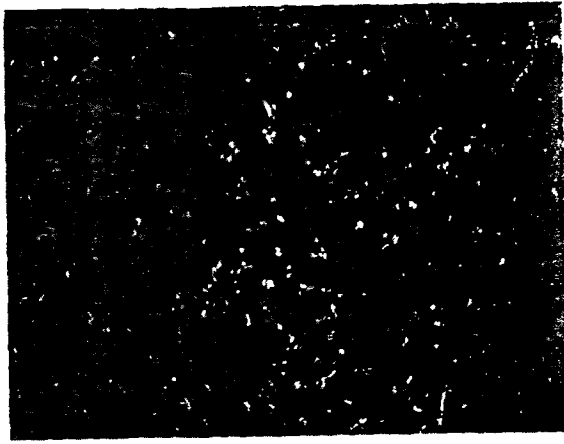


Fig.19 Microscopic observations after 15-minute KOH-H₂O etching. The degree of etching increases with the increase of Si fraction of the films, which corresponds to the order from top to bottom. The amplification is 110x.

4.CONCLUSIONS

It has been demonstrated in this study on the LPCVD of amorphous and crystal SiC that DES is a safe, easily delivered and suitable source for low temperature LPCVD silicon carbide films. Amorphous SiC thin films and crystalline cubic-SiC material have been deposited below and higher than 850C, respectively. The activation energy and a reaction mechanism involving the production and subsequent desorption of diethylsilene have been suggested, which explain the observed deposition dependency with the temperature and input pressure. It has been suggested that gas phase polymerization occurs at the DES input pressure above 0.05 torr(at 700C) or temperature above 700C(at 0.2 torr). The effect of the degree of polymerization on both the mass transfer coefficient and the diffusivity of a polymer (and thus on the Sherwood number) has been elaborated theoretically. Qualitative agreement between the predicted and observed morphology of the deposited films was obtained, that is , low temperature and pressure are strongly recommended. In an etching study, Si fraction of the films has been found to be effective on the ability for the films to prevent etching and a hypothesis, in which the silicon in amorphous SiC can react with KOH:H₂O etching solution and a porous film is formed after the etching, has been proposed. In the film evaluation, the film's chemical compositions, bonding and crystallinity were determined by RBS, IR and x-ray diffraction, respectively. The hydrogen content in the films can be ignored as shown as IR data.

ACKNOWLEDGEMENTS

The author wishes to thank Dr. Grow and Dr. Levy for their instruction in this study.

References:

1. P.T.B. Shaffer, *Acta. Crystallogr.*, Sect. B, 25, 477(1969).
2. W.F. Knippenberg, *Philips Res, Rep.*, 18, 161(1963)
3. J.A. Lely, *Ber. Dent, Keram Ges*, 32, 229(1970)
4. P. Rai-Choudhury and N.P. Formigoni, *J. Electrochem. Soc.* 116, 1440(1969)
5. J.M.Harris, H.C. Gatos, and A.F. Witt, *J. Electrochem. Soc.*, 118, 335, 338 (1971)
6. R.W. Brander, in *Silicon Carbide*, 1973, edited by R.C. Marshall, J.W. Faust and C.E. Ryan (University of South Carolina Press, Columbia, 1974).
7. W.B. White, W.M. Johnson, and G.B. Dantzig, *J. chem. Phys.* 28, 751(1985)
8. G. Eriksson, *Chemica Scripta* 8, 100(1975)
9. J.M. Harris, H.C. Gatos and A.F. Witt, *J. Electrochem. Soc.* 118 No.2, (1971) 338
10. T.J. Lewis, *Mater. Res. Bull.*, 4, 321(1969)
11. W.A.P. Claassen, J. Bloem et al, *J. Crystal Growth* 57(1982) 259-266
12. C.H.J. Van den brekel and L.J.M. Bollen, *J. Crystal Growth* 54, (1981) 310
13. Karl J. Sledek, *J. Electrochem. Soc.* 118, No.4, (1971) 654
14. H.J. Kim, J.A. Edmond, J. Ryu, H. Kong et al, *1-st International SAMPE Electronics Conference, June 23-25, (1987).* 370
15. S.Yoshida et al, *J. Appl. Phys.* 62(1), 1 July 1987
16. J.Anthony Powell et al, *J. Electrochem. Soc.* 134 No.6, (1987) 1558
17. P.Liaw and R.F. Davis, *J. Electrochem. Soc.* 132, No.3 (1985) 642
18. Y.Furumura et al, *J. Electrochem. Soc.* 135, No.5 (1988) 1255
19. Z.C.Feng and A.J.Mascarenhas, *J. Appl. Phys.* 64(6) sept.1988(3176)
20. J. A. Lely, *Ber. Deut. Keram. Ges.*, 32, 229(1955).
21. S.Nishino et al, *J. Electrochem. Soc.* 127. No.12, (1980) 2674
22. Kawamura, T.; Yamamoto, N. In "Amorphous Semiconductor Technologies and Devices 1982"

23. Mark A. Petrich, *Chemtech*, December 1989, (740)
24. S.Nishino et al, *J.Electrochem. Soc.* 127, 2674(1980)
25. R.C. Ellis, Jr., *ibid.*, 420
26. J.A. Edmond, J.W. Palmour, and R.F. Davis, *J. Electrochem. Soc.* 133 (1986), 650
27. Stanley Middleman and Andrew Yeckel, *J.Electrochem. Soc.* 133, (1986),1951
28. C.G. Newman, H.E.O'Neal, M.A. Ring, F. Leska and N.Shipley, *Intern. J chem. Kinetics* 11 (1979)1167
29. M.J.Mc Geary (Research Center, Olin Corporation, CT 06410-0586), *Private Correspondence to Dr. Grow*, Mar. 1991
30. T.U.M.S. Murthy et al, *J. Crystal Growth* 33, (1976) 1
31. *Encyclopedia of Chemical Technology*, third edition 20 (John Wiley & Sons, Inc.)
32. M. Fatemi and P.E.R. Nordquist, *J. Appl. Phys.* 61(5), 1 March 1987 1883

Appendices

Experimental conditions

Wafer ID number	Temperature (C)	Pressure (torr)	Flow rate (SCCM)
Y3			
Y4	700	0.2	30
Y5			
Y7			
Y8	650	0.2	30
Y9			
Y10			
Y11	700	0.2	50
Y12			
Y14			
Y16	600	0.2	30
Y18			
Y13			
Y19	700	0.2	10
Y20			
Y21			
Y22	700	0.2	20
Y24			
Y26			
Y29 (Quartz)	700	0.2	40
Y27			
Y28			
Y30	750	0.2	30
Y31			
Y32			
Y33	800	0.2	30
Y34			
Y35			
Y36	700	0.1	30
Y37			
Y38			
Y39	700	0.05	30
Y40			

Y47			
Y48	700	0.15	30
Y49			
Y50			
Y51	700	0.3	30
Y52			
Y50'			
Y51'	700	0.25	30
Y52'			
Y53			
Y54	675	0.2	30
Y55			
Y56			
Y57	850	0.2	30
Y58			

Temperature dependence of deposition rate

Temperature (C)	600	650	675	700	750	800	850
$\frac{1000}{\text{Temperature (K}^{-1}\text{)}}$	1.145	1.083	1.055	1.028	0.978	0.932	0.890
Deposition Rate (Z=1, 2, 3) (mg/hr)	1.58 1.54 1.43	6.35 5.98 5.60	10.40 9.67 9.47	18.40 17.50 15.00	23.36 20.71 18.22	21.40 18.00 14.40	45.70 35.95 27.15
Deposition Rate (mg/hr) (Average)	1.517	5.976	9.845	16.97	20.76	17.93	36.27
Ln(D.R.)	0.417	1.788	2.287	2.831	3.033	2.887	3.591

Note: The flow rate and input pressure are 30 SCCM and 0.2 torr, respectively.

The relationship between deposition rate and flow rate

Flow rate(SCCM)	10	20	30	40	50
Deposition rate(Z=1, 2, 3) (mg/hr)	7.78	12.85	18.40	21.90	23.30
	6.67	11.23	17.50	18.65	20.60
	6.00	10.05	15.00	21.55	18.10
Deposition rate(Ave. mg/hr)	6.82	11.38	16.97	*	20.67

Note: The temperature is 700C and pressure is 0.2 torr.

*: In the run with the flow rate of 40 SCCM, one quartz wafer was used so that the average deposition rate on (100) Si wafer can not be obtained.

The relationship between deposition rate and input pressure

Input pressure (torr)	0.05	0.10	0.15	0.20	0.25	0.30
Deposition rate (Z=1, 2, 3)	3.33	7.96	13.80	18.40	18.37	17.70
	3.48	7.46	12.87	17.50	17.23	16.60
	3.33	6.67	11.50	15.00	15.67	15.20
Deposition rate (Ave. mg/h)	3.380	7.363	12.72	16.97	17.09	16.50

Note: The temperature is 700C and flow rate is 30 SCCM.

The relationship between radial thickness variation(Average on the three wafers) and input pressure

Pressure	Radial Thickness Variation(%)
0.05	3.3048
0.10	5.8965
0.15	4.7631
0.20	4.4428
0.25	3.7270
0.30	3.2485

Note: Radial thickness variation = $100 * (d_{max} - d_{min}) / (d_{max} + d_{min})$, where d_{max} and d_{min} are the maximum and minimum film thickness measured in the wafer center and 10 mm from the wafer edge. Temperature = 700C, Flow rate = 30 SCCM.

The relationship between radial thickness variation and deposition temperature

Temperature	Radial Thickness Variation
650	3.1505
700	4.4428
750	5.6411
800	5.5490
850	3.7554

Note: The data of the film deposited at 600C have been ignored because of the too thin film.

Pressure = 0.2 torr, Flow rate = 30 SCCM.

The relationship between radial thickness variation and flow rate

Flow rate	Radial Thickness Variation
20	4.1565
30	4.4428
50	4.4872

Note: The data of the film deposited on flow rate 10 SCCM and 40SCCM have been ignored because of the too thin film and the quartz used, respectively.
Pressure = 0.2 torr, Temperature = 700C.

The relationship between chemical composition and deposition temperature

CVD temperature (C)	Chemical composition	
	Si	C
600	0.50	0.50
650	0.73	0.27
700	0.63	0.37
750	0.565	0.435
800	0.67	0.33
850	0.45	0.55

Note: Pressure = 0.2 torr, Flow rate = 30 SCCM

The relationship between chemical composition and deposition pressure

CVD pressure(torr)	Chemical composition	
	si	C
0.05	0.60	0.40
0.10	0.55	0.45
0.15	0.57	0.43
0.20	0.63	0.37
0.25	0.64	0.36
0.30	0.60	0.40

Note: Temperature = 700C, Flow rate = 30 SCCM.

The relationship between chemical composition and flow rate

Flow rate (SCCM)	Chemical composition	
	Si	C
10	0.73	0.27
20	0.57	0.43
30	0.63	0.37
40	0.575	0.425
50	0.62	0.38

Note: Temperature = 700C, Pressure = 0.2 torr.

Data of the mass, average thickness and density of the films

Wafer ID number	Mass (on both sides) (mg)	Average thickness (A)	Density (g/cm³)
Y3	55.2	16333	2.15
Y7	25.4	8013	2.02
Y10	69.8	21536	2.06
Y14	12.6	3828	2.10
Y21	51.4	16894	1.94
Y26	43.8	11233.4	2.48
Y28	59.1	15102.5	2.49
Y32	42.8	11146	2.45
Y35	23.9	6863	2.22
Y38	20.0	5377	2.37
Y50	53.0	17496.8	1.93
Y53	31.2	11038.4	1.80
Y56	91.4	22610.6	2.57

Note: The index of refraction was taken as 2.80 in the measurement of the thickness in the Nanospec interferometer.

Etching data

Wafer ID number	The difference of masses between before etching and after etching $\frac{WB - WA}{WB} * 100$	Si fraction
Y16	0.0459	0.5
Y4	0.7343	0.63
Y30	0.9275	0.565
Y33	1.4400	0.67
Y8	2.9400	0.73

Note: Pressure = 0.2 torr, Flow rate = 30 SCCM.